EVOLUTION OF THE OCEANIC LITHOSPHERE AND SHEAR WAVE TRAVEL TIME RESIDUALS FROM OCEANIC EARTHQUAKES

by

JEREMY D. DUSCHENES

B.Sc., LOYOLA OF MONTREAL

1975

SUBMITTED IN PARTIAL FULFILLMENT

OF THE REQUIREMENTS FOR THE

DEGREE OF MASTER OF

SCIENCE

at the

MASSACHUSETTS INSTITUTE OF

TECHNOLOGY

August, 1976

Signature of the Author .....
Department of Earth and Planetary Sciences,
August 9, 1976

Certified by .....
Thesis Supervisor

Accepted by .....
Chairman, Departmental Committee
on Graduate Students

ABSTRACT

EVOLUTION OF THE OCEANIC LITHOSPHERE AND
SHEAR WAVE TRAVEL TIME RESIDUALS
FROM OCEANIC EARTHQUAKES

by

JEREMY D. DUSCHENES

Submitted to
the Department of Earth and Planetary Sciences
on August 9, 1976
in partial fulfillment of the requirements
for the degree of Master of Science

Shear wave travel time residuals have been measured for 24 oceanic earthquakes, including normal faulting events on ridge crests and intraplate events. The data, plotted against $\sqrt{age}$ of the lithosphere in which the event occurred, show a decrease in residual of 6±1 seconds from ridge crest to oceanic lithosphere 100 m.y. old. This decrease is caused by an increase in shear velocity within the upper mantle as a function of lithospheric age. Modelling of the upper mantle, using seismic velocities, a standard thermal model for the spreading lithosphere, and published phase diagrams for dry and wet versions of gabbro-eclogite, and peridotite, was done in an attempt to produce a residual curve similar to that observed. Comparison of the predicted and observed residuals indicates that the mantle cannot be dry, but is unable to distinguish between the wet systems, principally because of the large number of assumptions involved in modelling velocity changes across phase boundaries. However, the wet gabbro-eclogite model is unable to satisfy constraints on absolute local shear velocity imposed by surface wave analysis, and a peridotitic upper mantle is favoured. An azimuthal variation of residual, correlative with shear wave attenuation data, exists for an event along the Gibbs Fracture Zone and is related to the high lateral velocity gradient within very young lithosphere.

A study of short period records shows that there is a small arrival shortly after, and of opposite polarity to, P, common to many of these events. This arrival has been interpreted as pP, indicating that the events are uniformly shallower than 15 kilometers, a conclusion corroborated by the surface wave analysis on some of these events, of other authors.

Thesis Supervisor: Sean C. Solomon
Assistant Professor of Geophysics

TABLE OF CONTENTS

ACNOWLEGEMENTS

I am very grateful to my thesis supervisor, Sean Solomon, for having suggested this topic, and for his help at all stages of completion of the work. Special thanks to Bob Siegfried, Peter Bird, Randy Richardson, and Gene Simmons, for their cheerful willingness to answer my many questions. Last but not least, thanks to Mike Fehler, Shamita Das, and Steve Taylor, whose good humour was always contageous.

This research was partially supported by the National Science Foundation under NSF Grant DES75-14812.

INTRODUCTION

The theory of plate tectonics postulates that plates are created at mid-oceanic ridges and are subsequently destroyed in subduction zones (e.g., LePichon,1968; Morgan, 1968). Studies in recent years have shown that several properties of the oceanic lithosphere change as it moves out from the ridge. These include depth of the sea floor below sea level (e.g., Sclater et al.,1971), heat flow (e.g., Parsons and Sclater,1976), and seismic velocity (e.g., Kausel et al.,1974). The concern in the present study is with the change of shear wave velocity in the oceanic lithosphere as a function of age.

Both surface and body waves have been shown to travel at varying velocities in the oceanic lithosphere, and with minor unsubstantiated exceptions (Hart and Press,1973), higher velocities are found farther from the ridge, below older sea floor. Forsyth (1975), Kausel et al. (1974), and others have shown that Rayleigh waves increase markedly in phase velocity with age across the Pacific. Hart and Press (1973) have shown similar results for Sn in the Atlantic. On a gross scale, this increase has been attributed to the cooling of the upper mantle with time, and attendant changes in physical properties affecting seismic velocity.

In nearly all cases, the seismic waves studied have been those moving horizontally through the lithosphere along the surface of the earth. The biggest problem in using such waves to discern lateral variation of velocity is to calculate the effects of each segment of the wave path where the wave has moved through lithosphere of varying age. This has been accomplished using the "pure path" technique (Forsyth,1975), in which an ocean basin is regionalized into zones of equal age, and the wave paths are divided into fractional times spent in each zone.

A second approach has been to study body waves, which by travelling more nearly vertically, only pass through lithosphere of one specific age. This technique has been used in the study of S waves (Girardin and Poupinet, 1974), ScS and multiple ScS waves (Sipkin and Jordan, 1975,1976), and is used in the present study. An inherent disadvantage in this technique is that the waves spend only a fraction of their travel time in the upper mantle. As a result, absolute velocities in this zone cannot be directly inferred since velocities along deeper parts of the ray path are not accurately known. However, relative travel times can be measured, and by making assumptions about velocity homogeneity in the middle and lower mantle, velocity anomalies in the upper mantle can be isolated. (For the purposes of this paper, the term

"upper mantle" will be used to refer to the outermost 100 kilometers of the earth. The lithosphere-asthenosphere boundary is taken to be the top of the low velocity zone.)

Nearly all changes in the upper mantle as a function of age, including contraction, phase change, and heat flow variation, are in some way caused by conductive and convective cooling. Variation in shear velocity is a sensitive indicator of lithospheric aging because it is greatly affected by the degree of partial melting in a rock. Given a specific composition, (ie. rock type and fluid content), partial melting at a given depth is primarily a function of temperature. Conversely, given a temperature field, partial melting, and hence shear velocity is a function of composition and fluid content. In modelling the upper mantle in this study, the latter approach has been used.

Twenty-five shallow earthquakes along mid-oceanic ridges and within oceanic parts of the plates have been examined and relative travel times of shear waves measured. A curve of shear wave travel time residual with respect to the Jeffreys-Bullen tables versus age has been constructed. A particular petrologic-velocity model of the upper mantle, which satisfies shear velocity data from this and other studies is presented.

MEASUREMENT OF TRAVEL TIME RESIDUALS

Two types of earthquakes have been considered in the present study: normal faulting events along mid-ocean ridges, and intraplate earthquakes occurring within the oceanic plates, away from plate boundaries. All events along transform faults, except one, have been deliberately avoided, since the age of the lithosphere is generally different on each side of such faults. Table 1 lists the pertinent data of the events studied and Figure 1 shows their location. This list is considered exhaustive for the period 1964-1972. All other seemingly useful events are either too small, are overshadowed in the records by larger events, or have imprecise origin times, making residual calculations pointless.

SH arrivals were measured from long period WWSSN seismograms for each event from as many stations as possible within the distance range of 30° to 70°. 30° was taken as the lower limit, to avoid the possibility of using arrivals of which the S wave had travelled through the laterally heterogeneous lithosphere at too oblique an angle, or which, because of horizontally layered transition zones in the upper mantle, may not have travelled along ray paths predicted by the Jeffreys-Bullen travel time tables. Beyond 70°, the S phase has

an arrival time too close to those of several other phases, notably SKS, ScS, and SP. The arrivals were subjectively rated on a scale of 1 to 4, depending on the sharpness of the arrival and the clarity of the seismogram. Figure 2 shows a sampling of typical S waves and their subjective ratings.

Using International Seismological Center data for origin time, epicentral location, and depth, shear wave travel time residuals with respect to the Jeffreys-Bullen travel time tables were calculated from the S wave arrival times. Two corrections were applied to the data, one for the ellipticity of the earth, the other for local geological effects below the receiving stations. The ellipticity corrections were drawn from the tables of Bullen (1937), which were expanded in a manner described in Appendix 1, so as to cover a larger portion of the earth than does the original reference.

The station corrections calculated by Sengupta (1975) were applied to compensate for velocity heterogeneities below each WWSSN station. The merit in applying these corrections can be seen in Figure 3, the residuals from event 20, plotted as histograms before and after applying the corrections.

All events were standardized to a depth of 10 kilometers below sea level to facilitate comparison of the residuals. This was done by simultaneously altering

the origin time and depth, thus changing the P and S travel times. The computations were all made with respect to the Jeffreys-Bullen travel time tables. This procedure was followed because the earthquakes studied are in general not deeper than 15 kilometers below sea level, and the ISC depths are considered inaccurate for shallow events. The validity of this statement will be discussed more fully later.

DISCUSSION OF THE RESIDUALS

The histogram of residuals for each of the first 24 events studied is presented in Figure 4. From most of these histograms, a single value of the residual has, in a very subjective manner, been selected. The mode, median, mean, rating distribution, and number of arrivals for each event has been taken into account. The residual estimated by this method is the value considered to be most representative, given the distribution, quality, and quantity of the data from each event.

These residuals are plotted in Figures 5, 6, and 7, against the square root of the age of the lithosphere in which the respective event occurred. The error bars delineate subjective limits of the possible residual, and are some indication of the closeness to which a set of data resembles a Gaussian distribution of low variability.

Error bars in the ages are also somewhat subjective, but at the same time are a reflection on how well the magnetic anomaly pattern on the sea floor has been established. The time scale proposed by Sclater *et al.* (1974) has been used to convert anomaly number to age.

The distribution of data in some of the histograms in Figure 4 is too scattered to give a representative residual value. Others give residuals which because of

complicated sources or near-source structure are grossly inconsistent with residuals from other events in lithosphere of similar age. Six events among the 24 studied fall into this category and have been eliminated from the residual versus age plots. They are:

1) Event 5: The histogram has a double peak with modes at -1.5 and 4 seconds. It is possible that the travel times have been affected in an undetermined fashion by the deep structure of the nearby Puerto Rico Trench. There is however, no correlation of residual with azimuth. A residual taken from the higher mode, 4 seconds, would fit reasonably well in Figure 5, but such a value cannot honestly be retrieved from the histogram.

2) Event 8: The scatter from this event seems random. A residual of 5 seconds, corresponding to the single greatest concentration of points on the histogram, would fit well in Figure 5, but again the value is statistically meaningless. Cause of the scatter is unknown.

3) Events 21 and 22: Both of these occurred very close to the Tonga Trench. The stations which detected S waves are mostly in Australia. The waves therefore likely passed through the subduction zone behind the Tonga Trench, and encountered higher than normal velocities in the cooler subducting slab, which lowered the residuals. Since the waves were not passing through "normal" asthenosphere, these events have been eliminated.

4) Event 23: This is the most puzzling of all the events because it occurred in apparently normal oceanic lithosphere of well determined age, and yet gives a well distributed peak of residuals high above the value expected for that age on the basis of all other data. With no other suitable earthquakes within, or at nearby edges of this plate from which to study travel times, it is not possible to ascertain whether the high residual is characteristic of the region or whether a local thermal anomaly in the upper mantle, which might slow the waves down, near source, is to blame. While it is possible that the Peru-Chile Trench and the Andean Cordillera had an effect on the times, not accounted for by the station corrections, since 6 of the 7 arrivals measured were from stations in South America and the Caribbean, it is significant to note that the residual measured at RAR, in the opposite direction, is also in the 10 to 12 second range.

5) Event 24: This event produced a highly scattered set of low residuals. The low average value may be the result of the extremely low spreading rate which would tend to depress the isotherms at the ridge, and raise the velocities. This does not account for the scatter.

By superimposing Figures 5, 6, and 7, the residuals for the Atlantic and Pacific events can be seen to fit the same curve. The Indian Ocean events do not fit,

although the change of residual with age is the same. There is an offset of about 2 seconds between the curves for the Indian, and for the Atlantic and Pacific Oceans, which will be discussed later. For all three oceans, a decrease in residual of 5 to 7 seconds from ridge crest to oceanic lithosphere older than about 100 m.y. is apparent. The combined data is presented in Figure 8, with all Indian Ocean residuals increased by 2 seconds. The aim of the present study is to explain the variation of S wave travel time residuals with age of the lithosphere in which the event occurred.

Residuals can be created at any point along the ray path (e.g., Cleary and Hales,1966), but the effect of velocity heterogeneity below individual receiving stations has already been corrected for by the application of station residuals. The portion of each ray path below a depth of 100 kilometers will be assumed to contribute negligibly and randomly to the relative residuals. That this is a valid assumption is perhaps questionable in view of the lateral shear velocity heterogeneity apparently observed in the lower mantle (e.g., Julian and Sengupta, 1973), but if these inhomogeneities are relatively small compared to the area within which the rays spread out from an event, then the effect will be to scatter the distribution of the data slightly. This may account for some of the poor distributions noted in

Figure 4. It will be shown that with reasonable assumptions on properties affecting shear wave velocities in the upper mantle, the observed variation of residuals can be adequately explained.

PREVIOUS WORK ON SHEAR WAVE DELAYS

Travel time delays of shear waves as a function of age of the oceanic lithosphere have been measured previously by other authors, using ScS and multiple ScS travel times (Sipkin and Jordan,1975,1976), and S travel times (Girardin and Poupinet,1974). The technique used by Girardin and Poupinet in estimating a residual for the Mid-Atlantic Ridge is the same as the one used in the present study, although their choice and manipulation of data is slightly less refined. The events used in their study were not all on the Mid-Atlantic Ridge, nor were they all normal faults. No station corrections were applied, and no attempt was made to correlate residual with age. All measured residuals were combined on one histogram which gave a mean value of 3.7 seconds at the ridge, relative to old lithosphere. This value is significantly lower than the 6±1 seconds observed in the present study. The discrepancy is likely caused by Girardin and Poupinet having diluted their ridge event residuals with data from events away from the ridge which have lower residuals, and having omitted station residuals.

Sipkin and Jordan (1976) have measured shear wave residuals by using ScS and multiple ScS arrivals. The residual created in the vicinity of a surface bounce point can be isolated by measuring arrivals of succesive phases

at the same station. If the assumption that the relative residuals measured in the present study are not created below 100 kilometers is correct, then it should be possible to match the slope of Sipkin and Jordan's curve with that in Figure 8. In fact a reasonable match can be made, but it is not significant, 1) because there is a lot of scatter in both diagrams, and 2) because Sipkin and Jordan have no residuals measured at bounce points in lithosphere younger than 15 m.y. which, in Figure 8, is where the greatest change of residuals with age occurs. Their extrapolation of the residual curve to the zero age axis is arbitrary, and that it gives a value at the ridge crest close to that of Girardin and Poupinet is of no statistical importance.

In summary, the shear wave residuals measured in this study are difficult to compare to those previously measured because of differences in the data sets, and ways in which the data were handled. Where data are comparable, no significant discrepancies exist.

VELOCITY STRUCTURE OF THE OCEANIC LITHOSPHERE

Although shear wave travel time delays are more important to the present study, in the modelling described in this section, P and S velocities, travel times, and delays, have had to be computed simultaneously, because the origin time, epicentral location, and depth, of each event studied has been obtained by a least squares method on the P arrivals. This is equivalent to assuming that the P residual is zero. If the conditions in the upper mantle are such that they create not only an S travel time delay, but also a P delay, then the latter must be subtracted from the former to give an S delay comparable to the ones measured.

Velocity in rock is determined by several parameters, principally mineralogy, temperature, pressure, degree of partial melting, and crack distribution. Degree of partial melting is a function of mineralogy, temperature, pressure, and fluid content. By specifying those 4 parameters at a given point in the upper mantle, and by ignoring the effects of microcracks which are likely closed at pressures above a few kilobars (Birch,1960), both shear and compressional velocities can be computed at that point.

The first problem is to map a temperature-pressure regime onto the upper mantle. The pressure gradient is fairly accurately established at 3.3 kilometers per kilobar. The temperature is not known at all precisely, and must be modelled. The equations of Sleep (1974), which incorporate a fixed temperature near the solidus at the base of a slab of constant thickness, have been used. In the computations, the temperature and thickness were taken as 1200° and 100 kilometers, respectively. The diffusivity of the rock was taken as .0066 cm^2/sec, and the adiabatic gradient was assumed to be small compared to the conductive gradient. The isotherms generated, and used in all the computations, are shown in Figure 9.

The composition of the mantle must also be modelled. Correlation of seismic properties with mantle petrologic models has been dealt with by several authors previously (e.g., Forsyth,1976; Hart and Press,1973). Forsyth and Press (1971) describe the technique used in the present study of applying phase diagrams directly to the lithosphere. Computations have been done for two phase diagrams, those of peridotite (Wyllie,1971a), and of gabbro-eclogite (Wyllie,1971b). Separate computations have been done for dry systems, and for wet systems containing traces (.01%) of water (Wyllie,1971a). The oceanic crust, which is petrologically dissimilar to the lithosphere, has been ignored in the calculations because it is very thin

with respect to the lithosphere, and seismic waves spend only a small amount of time passing through it.

Applying such phase diagrams to the lithosphere introduces some error, because most of the temperatures of the phase boundaries within these systems are not known experimentally to better accuracy than a few degrees, and several curves are extrapolations of insufficient numbers of data points.

Converting a given phase to a velocity involves perhaps the most imprecision of all the computations. In the solid field, the velocity of a polymineralic aggregate can be expressed as the sum of 4 terms:

$$V_{ps} = \sum_i x_i w_i v_{i_{ps}} + f(\eta_c, \eta_p) + \sum_i x_i \frac{\partial V_{ips}}{\partial T} + \sum_i x_i \frac{\partial V_{ips}}{\partial P}$$

The first term is the sum of the velocities of i component minerals, multiplied by their volume percentage, multiplied by a weighting factor. The second is a "crack" term, correcting the velocity for the effects of microcracks and pores in the rock. The third and fourth terms deal with changes of velocity as a function of temperature and pressure, disregarding phase changes.

The "crack" term can be ignored because at 10 kilometers depth, most of the cracks have closed, and the effect below that depth is negligible. Below 30 kilometers, ie. above 10 kilobars, all the cracks are believed closed, and the term vanishes (Birch, 1960).

Changes in velocity with temperature and pressure are only well known for a few minerals assumed to be in the mantle, and for a lack of data, a single value, applicable to all rocks, has been adopted. The pressure gradients used for Vp and Vs are .0029 km/sec/km and .0010 km/sec/km (Simmons and Wang,1971; Anderson and Lieberman,1969). The temperature gradients used are, respectively, -.0004 km/sec/°C and -.0003 km/sec/°C (same references). The effect of not using individual gradients for each mineral component is minor.

Calculation of the first term in the equation is possible because the velocity of individual minerals is well established. The accuracy of the term is dependent on the accuracy with which the modal composition is known. The exact modal composition, however, of any particular phase field, is not defined by the phase diagram, and somewhat vague estimates of relative mineral content must be used. This imprecision negates the advantages of applying any weighting scheme, ie. Voigt-Reuss, to the calculations. Modal compositions within the various fields have been taken from Ringwood (1975), Wyllie(1971b), and Green(1973). The velocities used are from Simmons and Wang (1971), Press (1966) and Simmons (unpublished material).

Through the combination of uncertainties, it is not possible to establish velocities within any of the

solid fields to better than about ±.15 km/sec. Far greater uncertainty is associated with the problem of establishing velocity changes across the hydrous and anhydrous solidi. Some data on velocity changes across phase boundaries do exist (Murase and McBirney,1973; Farberov et al.,1975), but measurements are few, and deal primarily with silica rich rocks which are relatively easy to handle at their melting temperatures in the 600°C to 800°C range. Measurement of velocity in partially molten mafic rocks is much more difficult because of the higher temperatures involved.

A velocity curve similar to one proposed by Solomon and Julian (1974) has been adopted for the purposes of the present study. In the dry systems, for a given pressure, the velocity in the solid field is assumed to decrease along the linear temperature gradient previously mentioned. At the solidus, the velocity decreases suddenly by a small percentage as the first minimal amount of partial melting occurs. Beyond the solidus, the velocity drops off as a cosine curve. The variables in the dry system, therefore, are the percentage drop in velocity at the solidus, the "wavelength" of the cosine curve over which the velocity drops, and the velocity at the lower end of the curve. Compressional velocity is assumed to drop by 5% across the solidus, and have a value of 4 km/sec at the lower end of the curve. The data of

Murase and McBirney (1971),and of Farberov et al. (1975), indicate that the cosine curve wavelength is in the range of 250°C to 400°C. A value of 300°C has been used in the computations for peridotite. For gabbro-eclogite, a much lower value must be used because, as seen in Figure 11b, the solidus and liquidus, or in the case of the wet system, the anhydrous solidus and the liquidus, are only separated by about 120°C. The length of the cosine curve cannot exceed this. The "wavelength" for Vp has been arbitrarily set at 120°C. No data suggests that the compressional velocity in a partially molten rock can drop quickly over such a small temperature range, and the concept is highly speculative, but the phase diagram seems to demand that such a phenomenon occur. The problem does not arise in the peridotite system, where the two pertinent phase boundaries are separated by more than 700°C.

Shear velocity, which is more sensitive to small amounts of partial melting, is assumed to drop 10% across the solidus, then decrease along a cosine curve similar to that for Vp but of shorter wavelength. The wavelength is assumed to be shorter because Vs drops to zero as soon as the rock loses its coherence and its capacity to sustain shear stress, whereas Vp is sensitive to the presence of detatched crystals in the melt. The shear velocity at the lower end of the curve is arbitrarily set at 2 km/sec, beyond which it drops immediately to 0 km/sec.

Arbitrary values of 150°C for peridotite, and 100°C for gabbro-eclogite, for the wavelength of the shear wave cosine curve, have been used.

In wet systems, the velocity is again assumed to decrease linearly along the appropriate temperature gradient in the solid field, but the sudden drop in velocity, as incipient melting begins, occurs at the hydrous solidus. Beyond this point, the velocity continues to decrease along the normal gradient until some temperature in the vicinity of the anhydrous solidus is reached, upon which the velocity, as in the dry system, drops off along a cosine curve. A fourth variable included in the calculations for wet systems is the offset, towards a lower temperature, of the beginning of the cosine curve from the anhydrous solidus. This variable is included because the presence of a small amount of water in the system is assumed not only to cause incipient melting at the hydrous solidus, but also cause more widespread melting before the anhydrous solidus is reached. The offset is assumed to be 50°C. Other variables have the same values as for the dry system. The velocity models used for peridotite are shown schematically in Figure 10. Those used for gabbro-eclogite are the same except that the length of the cosine curves for Vp and Vs is 120°C and 100°C, respectively.

The phase diagrams used in the computations are shown in figures 11a and 11b. The combination of any one of these, with the temperature map in Figure 9, and a pressure gradient of .3 kb/km results in a phase map of the upper mantle. The map derived using a wet peridotite phase diagram (Figure 11a) is presented in Figure 12. A grid of points superimposed on this phase map has been converted to velocities, shown in Figure 13, using the velocity model shown in Figure 10. Vertical travel times as a function of age have been determined by interpolation and integration over the 100 kilometers distance. To account for non-vertical travel paths of seismic waves within the upper mantle, the times were divided by cos 34°. 34° is the average angle of incidence for the distance range 30° to 70°, assuming an S velocity of 4.3 km/sec, and a P velocity of 8.0 km/sec. By subtracting, from the S travel time of any age, the P time for that same age, and the S time in 100 m.y. old lithosphere, a relative shear wave travel time delay versus age curve has been determined.

COMPARISON OF THE MODELS WITH OBSERVED RESIDUALS

The intention, in computing synthetic residuals, is to find a set of conditions in the upper mantle, ie. mineralogy, pressure, temperature, etc., which gives rise to a residual curve equivalent to the measured one. Unfortunately, because of the large number of variables and assumptions involved, no unique solution can be determined. However, the technique does allow the rejection of certain models and favours others.

In Figure 14, residual curves computed for a dry and a wet gabbro-eclogite upper mantle, using velocity models similar to those in Figure 10, but of shorter cosine curve, are shown. The calculation of residuals using these phase diagrams is somewhat pointless, because the phase maps analogous to Figure 12, generated as an intermediate step, indicate that the outermost lithosphere is eclogite, in direct conflict with observed sea floor rocks. In any case, the dry system doesn't produce a high enough residual at the ridge because not enough partial melting takes place. The wet system produces a reasonable fit to the observed curve, although it is slightly low at the ridge. However, the extremely speculative nature of the velocity model adopted for this particular phase diagram should be kept in mind in inter-

preting its residual curve.

Although consideration was given to doing the computations with pyrolite phase diagrams, the petrologic difference between the peridotite and pyrolite systems is vague, and as a result, the difference in computed residuals is not significant. The pyrolite model was proposed by Ringwood (1962) principally with the derivation by partial melting of a basaltic magma in mind, and its chemistry is more important than its mineralogy. However, velocities are not sensitive to minor differences in chemistry, and given the mineralogically vague quantitative nature of the phase diagrams, the two systems are, for the purposes here, essentially equivalent. The discussion below applies primarily to the peridotite phase diagrams which were actually used in the computations, but the results are very similar to those which would be obtained using the pyrolite model.

In Figure 15, residual curves are presented for dry and wet peridotite, using the velocity models in Figure 10. It is clear that a dry system cannot produce a high enough residual at the ridge for the temperature model assumed. The wet peridotite model provides a curve similar to that in Figure 8.

Close to the ridge axis, the residual curve can be changed by altering 1) the offset of the cosine curve from the anhydrous solidus, 2) the wavelength of the

cosine curve, 3) the change in velocity across the hydrous solidus, and 4) the velocity at the lower end of the cosine curve. Farther from the ridge, changing these parameters has less effect. The values used in the computations are highly speculative and may be erroneous.

Other parameters which have been kept fixed throughout the computations but whose values are somewhat arbitrary include the thickness of the slab, 100 kilometers, and the temperature at the base, 1200°C. By changing these, other values of the four velocity parameters can be used to create an acceptable residual curve.

Regardless, one main conclusion is clear. No reasonable set of variables can be combined with a phase diagram of any dry system to produce a residual curve similar to that observed. The same conclusion, that the mantle cannot be dry, has been reached by other authors, in studies for instance, of Q in the oceanic lithosphere (Solomon,1973), and petrologic evolution of the crust (Green,1971). The technique itself cannot resolve whether the lithosphere is wet gabbro-eclogite, wet peridotite, or wet pyrolite. However, the phase map indicates that it cannot be wet gabbro-eclogite, a conclusion reached by other authors, on the basis, among other criteria, of topographic variation with age, and petrology of rocks recovered from the sea floor (Forsyth and Press,1971). The assumptions involved in converting phases to velo-

cities are also much more highly speculative for gabbro than for peridotite.

In conclusion, the observed residual curve favours a wet peridotite or wet pyrolite mantle, though the gabbro-eclogite model cannot be rejected on shear wave residual grounds alone. The solution is non-unique, and will remain so, particularly until the effects on velocity in mafic and ultramafic rocks, of partial melting, is established.

COMPARISON OF THE MODELS WITH OBSERVED VELOCITIES

Delay times modelled are a reflection of relative changes in velocity with distance from the ridge. It is useful to see whether the velocity model proposed in Figure 13 using a wet peridotite phase diagram can satisfy absolute local shear velocity constraints established by other means.

Analysis of Sn waves travelling in the oceanic lithosphere has shown that Sn velocity averages 4.58±.02 km/sec below sea floor younger than 50 m.y., and 4.71±.01 km/sec below older sea floor (Hart and Press,1973). If Sn travels through the layer, above the asthenosphere, of highest S velocity, then the velocity model proposed in Figure 13 satisfies the data very well. Beyond 50 m.y., there is a continuous layer, in the spinel peridotite field, with a velocity of 4.7 km/sec. In younger lithosphere, the velocity is predominantly 4.5 km/sec and 4.6 km/sec, a combination of which will produce the proper average. The conclusion reached by the aforementioned authors, that the mantle cannot be strictly peridotite because no peridotitic phase has a shear velocity of 4.71 km/sec, is considered unjustified. The calculated velocities in the various phases are based on presently very vague knowledge of modal mantle mineralogy, and slight changes, for

instance, in the spinel content of spinel peridotite, can make an appreciable difference in the calculated aggregate velocity of the rock.

A second manner in which shear velocities in the oceanic lithosphere can be determined is by the inversion of surface wave data (Leeds et al.,1974; Forsyth,1975; Schlue and Knopoff,1976). Average velocities have been calculated by Forsyth in zones bounded by specific ages and depths. The agreement between these velocities, and similar ones calculated by arithmetic averaging of point velocities in similar depth-age blocks in Figure 13, shown in Table 2, is exceptionally good. Analogous velocities calculated for the gabbro-eclogite model are also shown in Table 2. Although that velocity model produces an acceptable residual curve, seen in Figure 14, it is obviously unable to satisfy absolute velocity constraints imposed by the surface wave inversion results.

The only deviation of significance between Forsyth's data and the peridotite model is for mantle deeper than 90 kilometers at 100 m.y., and between 20 and 45 kilometers at 20 m.y. and younger. The difference at 100 m.y. is caused by the difference in thermal models used, a slab with an isothermal base in the present study, versus a modified cooling half space in Forsyth's model. The difference in very young lithosphere is quite substantial, but in this zone where velocity changes rapidly both

horizontally and vertically, the interval over which the averaging takes place becomes critical, so the deviation is actually not significant.

Because of the variation of velocity with age, it is difficult to compare the velocity model in Figure 13 with studies, (e.g., Schlue and Knopoff,1976), in which analysis of Rayleigh and Love wave inversion provides average velocities across large age spans. Their average value for SH in the asthenosphere is higher than that shown in Figure 13, but the thermal model used in generating the velocity model dictates no change of velocity in the asthenosphere with age. As will be discussed later, this thermal constraint has no effect on the analysis and interpretation of the shear wave residuals. The technique used in the present study, which only involves SH waves, is not sensitive to the anisotropy in the asthenosphere measured by Schlue and Knopoff (1976).

Another check which can be made is to compare residual curves of velocity models generated by inversion of surface wave data, with the observed curve (Figure 8), and also with the modelled curve derived and favoured in the present study (Figure 15). Leeds et al. (1974) present a model of the spreading lithosphere in which Vp, Vs, and thickness as a function of age, are specified. The shear wave residual curve created by this model, shown in Figure 16, agrees well with those both in Figures 8 and 15.

The comparison is somewhat crude, because Leeds et al. (1974) quote average velocities over 10 to 15 m.y. age spans, and extrapolation of the curve to the ridge axis is purely hypothetical.

The velocity map in Figure 13, which assumes a peridotitic upper mantle, not only produces a good synthetic fit to the observed residual curve, but is also in agreement with models of the oceanic lithosphere (with which it can sensibly be compared) proposed to satisfy local absolute shear velocities measured with other techniques. The gabbro-eclogite model, although it creates an acceptable residual curve, is unable to satisfy these absolute velocity constraints, and can be rejected.

Agreement of the peridotite model with studies calculating the average shear velocity over very large age spans is not resolvable, given the lack of events in very old sea floor, and the differences in thermal models used in velocity modelling.

DEPTH DETERMINATION OF THE EVENTS STUDIED

Implicit in the discussions has been the assumption that the earthquakes studied are shallow, and that the shear waves travel through almost the full thickness of the lithosphere. This temporary assumption justified simultaneous alteration of depth and origin time to a standard 10 kilometers as previously described. If the depths calculated by ISC, and shown in Table 1, are correct, then the assumption is, in most cases, false. However, these depths, which are determined by a least squares method on P residuals, are suspect because 1) many have extremely large error bars, 2) the method is known to fail for some events in which case an arbitrary depth of 33 kilometers is quoted, and 3) more sophisticated depth determination techniques have yielded significantly dissimilar results.

There are two other methods of establishing the depth of oceanic events. One is through the analysis of surface wave phase velocities and amplitude spectra (Weidner and Aki,1973), the other is through the identification of depth phases such as pP, sP, pwP, and pwwP (Mendiguren,1971). Ideally the techniques should be used to compliment each other. Both have drawbacks. The surface wave analysis is a highly complex, time consuming

process, and the depth phase method is sometimes unreliable by itself, especially for shallow events where pP arrives soon after P and may be confusable with source effects.

Weidner and Aki (1973) have shown, using the surface wave technique, that two normal faulting events along the Mid-Atlantic Ridge, events 2 and 3 in this study, occurred at very shallow depths, about 3 kilometers beneath the ocean floor. Short period records have been examined in the hope of identifying phases similar to those found by Mendiguren (1971). Arrivals at 5 stations from event 2 are shown in Figure 17, with indication of phases which have been identified as P, pP, and pwP. An exact depth using these arrivals would be difficult to calculate because a continual trade-off occurs between the calculated depth and the model of crustal velocity, thickness, and water depth, used, but the pP arrival so soon after P implies a very shallow depth below the sea floor, on the order of 4 kilometers, in close agreement with Weidner and Aki's figure.

In Figure 18, short period seismograms from event 3 are presented. pP is easily identified, though later arrivals are not universally so, because of the poor quality of the records. The calculated depth from pP is about 2 kilometers below the sea floor, again in close agreement with the surface wave estimate. The model used

in generating approximate depth phase travel time tables is similar to that used by Mendiguren (1971).

From this evidence, all near-ridge events are concluded to be shallow, within the upper 15 kilometers of the lithosphere, and probably within the oceanic crust. The conclusion cannot be implicitly extrapolated to events in much older lithosphere. However, Mendiguren (1971) has applied a slightly less refined version of the surface wave technique to an event within the Nazca plate, and has corroborated his calculated depth of 9 kilometers below the sea floor, with depth phase arrivals. The depth determination technique used in the present study has been to look for short period arrivals soon after P, similar to those found by Mendiguren (1971) for an event away from the ridge crest, and those found in the present study for ridge crest events, shown in Figures 17 and 18. Such arrivals are shown for events 6 and 8 in Figures 19 and 20. Calculated depths are 3 and 1.5 kilometers below the sea floor, respectively. An attempt to apply the technique to event 7 failed, because the event appears to have a complex mechanism, and accurate P times are not measurable.

Of the 10 events in the Indian Ocean, 7 are close enough to either the Carlsberg or the Southeast Indian Ridge, that they are assumed to be shallow, from the work of Weidner and Aki (1973). Of the three remaining events,

the technique was applied to two, events 13 and 14. Event 15 was not tested because the origin time is imprecise, implying that source effects may be present on the seismograms soon after P. Event 14 yielded poor results because there were only 8 legible short period records among the WWSSN collection. The first depth phase recognizable may not in all cases have been pP, but all first arrivals indicate a depth of less than 10 kilometers below the ocean floor. Event 13 yielded slightly better data, of which 3 arrivals are shown in Figure 21. The calculated depth is 3 kilometers below the sea floor. At several stations, the P arrival was emergent, and could not be properly measured.

Both earthquakes in the Pacific, events 19 and 20, are assumed to be shallow because of their proximity to ridge crests. The depths calculated from Figures 17 through 21 are shown in Table 3, along with other depth estimations for the same events.

Depth phases are not reliable to use on individual events without corroborative data, because it is impossible to identify them unequivocally. Although pP, sP, pwP, and pwwP are theoretically the largest in amplitude of such phases, there are, in the case of shallow events, a large number of near source horizontal discontinuities at which reflection can occur, possibly generating a large number of minor phases. It is also virtually

impossible to tell depth phases from source effects for such events.

Although the phases identified in Figures 17 through 21 may have been misinterpreted, it is unlikely to be coincidental that these arrivals are common among several distant earthquakes, of which three are known to be shallow. It is also notable that the first arrival after P, pP, is almost exclusively of opposite polarity to P, as would be expected from a wave being reflected at a solid-liquid interface. That the arrivals may not be exactly at times predicted by any particular travel time table generated is a reflection on the velocity model used in calculating the theoretical travel times. Sediment thickness, sediment compaction, water depth, and crustal velocity, are all a function of lithospheric age, and none of those has been well established above particular epicenters. The minor inaccuracy in calculating depths from these phases is not important to the present study, because as long as the events are reasonably shallow, ie. less than 10 or 15 kilometers, the assumption permitting the standardization of the depths for comparison purposes is justified.

AZIMUTHAL VARIATION OF RESIDUAL

Transform fault strike-slip earthquakes have been deliberately avoided in measuring S wave travel time residuals because events in lithosphere of ambiguous age are not useful in constructing residual versus age curves. In many cases, there is a significant age difference between the lithosphere on opposite sides of the fault.

However, since the waves leaving an event on a transform fault do not all pass through lithosphere of the same age, it is interesting to see whether the residual curve shown in Figure 8 can successfully predict an azimuthal variation of residual. One transform event has been studied. It occurred on the northern edge of the Gibbs Fracture Zone, in the North Atlantic on Feb. 13, 1967, in an area where the fracture zone has a strike of about 95°, and where the age difference across the fault is approximately 25 m.y., the lithosphere being about 5 m.y. old to the north, and 30 m.y. old to the south (Pitman and Talwani,1972). If we assume that the transform fault has no effect on travel times, then from Figure 8, a residual of 6 seconds would be expected for waves travelling in the azimuth range 275° to 95°, and a residual of 4 seconds in the azimuth range 95° to 275°.

As shown in Figure 22, there is a strong correlation between azimuth and residual for this event, even though the azimuthal coverage is not complete. There are no WWSSN stations within the appropriate distance range to the north, in the Arctic, or to the southeast, in Africa. The most significant aspect of the distribution of residuals with azimuth is that all the waves travelling across the transform fault, or under the ridge have large residuals whereas those crossing neither feature have residuals in the range predicted by Figure 8. Because of the marked lateral velocity changes believed to exist below very young sea floor, the change of residual within the azimuth range 275° to 95°, ie. residuals of waves not crossing the transform fault, is understandable. A similar, though not as well defined, change of residual with azimuth exists for event 4 (see Figure 23), which occurred just west of the Mid-Atlantic Ridge. Waves travelling east from that event had to pass beneath the ridge, and have higher residuals than those travelling west.

There is a transition zone along the Gibbs Fracture Zone, in the azimuth range 260° to 275° from the epicenter, in which the spreading center to the north is truncated and is in direct contact with older lithosphere to the south. Neither the width, nor the upper mantle configuration, ie. isotherms, magma chamber shape and size,

convection pattern, of this zone, is known. Shear waves passing through it have uniformly high residuals. Heat flow surveys across the San Andreas Fault (Brune, 1969) have shown that no significant amount of shear heating occurs as the result of strike-slip movement along transform faults. It is therefore unlikely that the high residuals are a result of an anomalous degree of partial melting caused by shear heating in the transition zone. A possibility is that the segment of the ridge north of the transform fault is leaving a trail of hot asthenosphere behind it (Solomon, pers. comm.) beneath older lithosphere, as the whole Mid-Atlantic Ridge moves northward (Minster et al.,1974; Solomon et al.,1975), with respect to a fixed mesosphere. This concept is speculative to the extent that the relative motion of the asthenosphere and lithosphere is unknown, particularly at transform faults.

In the azimuth range 95° to 260°, only 2 arrivals have been recorded. Both residuals are significantly higher than predicted. The lack of data, and their poor quality, (both arrivals are rated 4, see Appendix 2), make interpretation of the residuals virtually impossible. It is obvious that the model of a thin transform fault separating two pieces of lithosphere of different ages, and not affecting the residuals, is not valid. Whether a trail of hot asthenosphere exists far enough south to

affect waves travelling at azimuths less than 260° is possible, but speculative.

Except for the two data points in South America, there is good correlation between residuals and differential shear wave attenuation measured by Solomon (1973), for the same event. Waves with high residuals, passing directly beneath the ridge, were also attenuated the most, whereas those travelling east have the lowest residuals and were attenuated least.

The possibility of azimuthal variation of residual existing directly as a function of lithospheric age is probably not good in the real world. It requires two conditions, neither of which is likely to be met. The first is that a thin transform fault must exist, seprating lithosphere of appreciably different age, but having no effect on travel time. The second is that lithosphere on both sides of the fault must be old enough not to contain appreciable lateral variation in velocity. However, it is inherent in the ridge transform fault system that active segments of such faults are between ridges, and hence in the vicinity of lateral velocity changes.

DISCUSSION OF DIFFERENCES IN RESIDUAL CURVES AMONG OCEANS

The calculation of residuals throughout this study has been made with respect to the Jeffreys-Bullen travel time tables. It has been assumed that no part of the decrease in residual of 6±1 seconds from ridge crest to old ocean is caused by conditions below a depth of 100 kilometers. The validity of this assumption seems confirmed by the fact that a combination of reasonable assumptions about the upper mantle gives rise to conditions which can create a residual equal to that observed. The absolute value of the residuals is of no concern, and merely reflects the slight non-adaptability of the Jeffreys-Bullen tables to the oceanic lithosphere. However, the offset of 2 seconds between the Indian Ocean curve (Figure 7) and the Atlantic and Pacific curves (Figures 5 and 6) remains a problem. The implication is that there is a constant difference in conditions affecting shear velocity beneath the oceans, below the 100 kilometer depth.

As a check that the difference is real, and not due to spurious station corrections, the arrival times at stations common to the Indian and Atlantic Oceans were studied. These included 15 stations in southern and eastern Africa, southeastern Europe, and the Middle-East.

If arrivals at these stations had been consistently late for events in the Indian Ocean, and/or consistently early for events in the Atlantic Ocean, there would have been indication that the difference was not real. However, the arrivals distribute evenly about the median for the Indian Ocean, and only very slightly below it for the Atlantic. The difference is therefore probably real, and caused by conditions below 100 kilometers.

It is beyond the scope of this study to examine velocity heterogeneity in the mantle below 100 kilometers, but there are certain differences between the Indian, and the Atlantic and Pacific Oceans, which may reflect differences at depth contributing to the offset. One such difference is in the magnetic anomaly pattern found on the ocean floor. In both the Atlantic and the Pacific, the pattern is straightforward, and spreading has been reasonably regular and calm over the last 100 m.y. In the Indian Ocean, the extremely complex, discontinuous, sea floor magnetic anomaly pattern indicates that spreading has been irregular and episodic. The cause is unknown presently, but the difference in spreading characteristics may reflect differences in the mantle thermal regime, affecting shear wave travel times.

A second difference is perhaps more subtle and more subject to interpretation, but Solomon et al. (1975) have shown that the Carlsberg and Southeast Indian Ridges are,

among spreading centers, two of the fastest moving, with respect to their "immediate source of new lithospheric material in the underlying mantle". A fixed mantle reference frame with which absolute plate motion can be measured (e.g., Morgan,1972) is extremely difficult to establish, but if Indian Ocean lithosphere is overriding cooler mantle at an anomalously fast rate, shear waves will encounter lower than normal temperatures, higher than normal velocities, and will have lower residuals. A difference of 2 seconds out of the whole travel time of the shear waves is very small, so that the perturbation could be extremely slight but extensive below the Indian Ocean.

Correlation between the complex magnetic pattern, the fast movement with respect to the underlying mantle source, and the offset in residual curves is purely speculative, and will remain so until the causes and effects of the Indian Ocean's complex past history are more fully understood.

CONCLUSIONS

If the base of the lithosphere is defined as the uppermost limit of partial melting and low velocity in the upper mantle, then shear velocity, which is very sensitive to partial melting, can become a good indicator of lithospheric growth. Travel time residuals from oceanic earthquakes indicate that velocity beneath very young sea floor is lower than that below old sea floor. A decrease in residual from ridge crest to lithosphere 100 m.y. old of 6±1 seconds exists for all oceans.

Velocity models of the outermost 100 kilometers of the earth have been computed using the thermal model of Sleep (1974). The most acceptable one is that of a wet peridotite or wet pyrolite upper mantle. The velocity data does not distinguish between the two since their difference is primarily chemical. The residual data strongly indicates that the upper mantle cannot be dry, unless it is significantly hotter than presently believed, because the partial melting in a layer of decreasing thickness with age, which is the primary cause of the residual gradient, simply would not exist.

Cooling of the slab as it moves laterally away from the ridge is able to produce lateral changes in velocity which translate to relative vertical travel time delays.

Several assumptions must be made in the calculations, notably those about velocity drops across the hydrous and anhydrous solidi, causing the solution to be non-unique. Within the resolution of the technique, the shear wave residuals measured in this study agree with those measured previously. Apparent differences are artificial creations of poor manipulation, or lack, of data. The preferred model also satisfies data on local oceanic lithosphere shear velocities measured by Sn travel times and surface wave inversion.

A basic assumption in using shear wave residuals to measure changes in upper mantle velocity and lithospheric thickness, has been that oceanic events occur at shallow depths. This has been confirmed through the study of depth phase arrivals from these events, and comparison to similar arrivals from events for which the depth has been established by surface wave analysis.

The technique of measuring shear wave residuals from oceanic events is presently not sensitive to whether the oceanic lithosphere continues to thicken indefinitely until it is subducted. There are several reasons for this. First of all, there are not enough strong events recorded in old sea floor from which to observe measurable waves. Those that are, such as events 21 and 22, are generally distant from seismic stations, or have poor azimuthal coverage. Secondly, the age of old oceanic

lithosphere is poorly defined, in part because of the Cretaceous "quiet zone", in part because of the increased inaccuracy of the dating process with age. Thirdly, the residual gradient decreases with age. Even if the lithosphere does continue to thicken with age, the change in properties affecting shear wave velocity in old lithosphere is likely very slow. The inaccuracies and assumptions presently involved in calculating shear wave residuals are such that small changes of residual in old lithosphere are beyond the resolution of the technique. These inaccuracies are a combination of inability to measure S wave arrivals properly because they are emergent or because of poor quality seismograms, possibly invalid assumptions about lateral velocity homogeneity in the mantle, especially under the Indian Ocean, and poor values of station residuals which in some cases are not based on enough data.

That the quality and quantity of the data precludes the possibility of resolving changes of residual in very old lithosphere justifies use of the thermal model included in the computations, a slab with an isothermal base. Forsyth (1976) has shown that in sea floor younger than 50 m.y., the slab and half space models are virtually indistinguishable. Since it is in this zone that the greatest change of residual with age occurs, the slab model is acceptable. If velocities do increase

indefinitely with age, they do so at a rate that is imperceptably slow, given the resolution and extent of the data.

Future work using shear wave travel time residuals as indicators of lithospheric growth is dependent on three conditions: 1) The occurrence of more oceanic intraplate earthquakes, particularly in parts of the ocean basins where the lithosphere is old but of well established age. 2) The better isolation of the part of the residual created near source. This involves the establishment of more accurate station residuals, based on more data. Some corrections quoted by Sengupta (1975) are based on only one or two measurements. Others have very large standard deviations. Although on the whole, the application of these residuals acts to reduce the scatter on the distribution of data, some values, notably that for NAI (Nairobi, Kenya), which consistently causes Nairobi to have the lowest corrected residual within a data set, are likely wrong. A more accurate estimation of these residuals will also permit better assessment of the reality of the Indian-Atlantic & Pacific offset in residual curves. The assumption made about velocity homogeneity in the mantle below 100 kilometers can certainly be refined also. 3) Velocity changes across phase boundaries of mafic rocks must be measured. This is largely a technical problem of developing a method

of measuring velocities in very hot, partially molten, materials. The assumptions made about velocity drops across the solidi are the most speculative of all in the development of a velocity model and synthetic residual curve.

In summary, the measurement of teleseismic shear wave travel times and computation of residuals is a good indicator of change of velocity in the upper mantle with lithospheric age. Resolution of the technique is limited principally by lack of knowledge on shear velocities in deeper parts of the mantle, and the effect of partial melting on velocity in mafic and ultramafic rocks.

REFERENCES

Anderson, O.L., and R.C. Liebermann, Elastic components of oxide compounds used to estimate the properties of the earth's interior, in: The application of modern physics to the earth and planetary interiors, ed. S.K. Runcorn, J.Wiley & Sons, N.Y., 425-448, 1969.

Anderson, R.N., D.A. Clague, et al., Petrology and magnetization of Basalts along the Galapagos spreading center, (abstr.) Eos Trans. AGU, 55, 298, 1974.

Banghar, A.R., and L.R. Sykes, Focal Mechanisms of earthquakes in the Indian Ocean and adjacent regions, J.Geophys. Res., 74, 632-649, 1969.

Birch, F., The velocity of compressional waves in rocks to 10 kilobars, part 1, J. Geophys. Res., 65, 1083-1102, 1960.

Brune, J.N., Seismicity, rate of slip, and heat flow along the San Andreas Fault in California, (abstr.) Eos Trans. AGU, 50, 384, 1969.

Bullen, K.E., The ellipticity corrections to travel times of P and S earthquake waves, Geophys. J. Roy. Astr. Soc., 4, 143-157, 1937.

Cleary, J., and A.L. Hales, An analysis of the travel times of P waves to North American stations, in the distance range 32° to 100°, Bull. Seismol. Soc. Amer., 56, 367-489, 1966.

Farberov, A.I., L.N. Sokolov, A.I. Levykin, S.I. Zubkov, and V.A. Yermakov, Measurements of ultrasound velocity and attenuation in partially and completely molten effusives, Doklady Akad. Nauk. SSSR, 220, 15-18, 1975.

Forsyth, D.W., and F. Press, Geophysical testing of petrological models of the spreading lithosphere, J. Geophys. Res., 76, 7963-7979, 1971.

Forsyth, D.W., The early strutural evolution and anisotropy of the oceanic upper mantle, Geophys. J. Roy. Astr. Soc., 43, 103-162, 1975.

Forsyth, D.W., The evolution of the upper mantle beneath mid-oceanic ridges, Preprint, 1976.

Girardin, N, and G. Poupinet, Teleseismic S travel time delay for Mid-Atlantic Ridge Earthquakes, Phys. Earth & Planet. Inter., 9, 303-313, 1974.

Green, D.H., Composition of basaltic magmas as indicators of conditions of origin - application to oceanic volcanism, Phil. Trans. Roy. Soc. Lon., Series A, 268, 707-725, 1971.

Green, D.H., Experimental melting studies on a model upper mantle composition at high pressure under H_2O saturated and H_2O undersaturated conditions, Earth Planet. Sci. Lett., 19, 37-53, 1973.

Hart, R.S., and F. Press, S_n velocities and the composition of the lithosphere in the regionalized Atlantic, J. Geophys. Res., 78, 407-411, 1973.

Julian, B.R., and M.K. Sengupta, Seismic travel time evidence for lateral inhomogeneity in the deep mantle, Nature, 242, 443-447, 1973.

Kausel,E.G., A.R. Leeds, and L. Knopoff, Variations of Rayleigh wave phase velocities across the Pacific Ocean, Science, 186, 139-141, 1974.

Leeds, A.R., L. Knopoff, and E.G. Kausel, Variation of upper mantle structure under the Pacific Ocean, Science, 186, 141-143, 1974.

LePichon, X., Sea floor spreading and continental drift, J. Geophys. Res., 73, 3661-3697, 1968.

McKenzie, D.P., and J.G. Sclater, The evolution of the Indian Ocean since the late Cretaceous, Geophys. J. Roy. Astr. Soc., 25, 437-528, 1971.

Mendiguren, J.A., Focal mechanism of a shock in the middle of the Nazca plate, J.Geophys. Res., 76, 3861-3879, 1971.

Minster, J.B., T.H. Jordan, and P. Molnar, Numerical modelling of instantaneous plate tectonics, Geophys. J. Roy. Astr. Soc., 36, 541-576, 1974.

Morgan, W.J., Rises, trenches, great faults, and crustal blocks, J. Geophys. Res., 73, 1959-1982, 1968.

Morgan, W.J., Deep mantle convection plumes and plate motion, Amer. Assoc. Petrol. Geol. Bull., 56, 202-213, 1972.

Murase, T., and A.R. McBirney, Properties of some common igneous rocks and their melts at high temperatures, Bull. Geol. Soc. Amer., 84, 3563-3592, 1973.

Parsons, B., and J.G. Sclater, An analysis of the variation of ocean floor heat flow and bathymetry with age, Geophys. J. Roy. Astr. Soc., in press, 1976.

Pitman, W.C., R.L. Larson, and E.M. Herron, Map of magnetic lineations of the world, Geol. Soc. Amer., 1974.

Pitman, W.C., and M. Talwani, Sea floor spreading in the North Atlantic, Bull. Geol. Soc. Amer., 83, 619-646, 1972.

Press, F., Seismic velocities, in: A handbook of physical constants, ed. S.P. Clark, Geol. Soc. Amer. Memoir 97, 195-218, 1966.

Ringwood, A.E., A model for the upper mantle, J. Geophys. Res., 67, 857-866, 1962.

Ringwood, A.E., Composition and petrology of the earth's mantle, McGraw-Hill, N.Y., 1975.

Schlue, J.W., and L. Knopoff, Shear wave anisotropy in the upper mantle of the Pacific Basin, Geophys. Res. Lett., 3, 359-362, 1976.

Sclater, J.G., R.N. Anderson, and M.L. Bell, The elevation of ridges and the evolution of the central Eastern Pacific, J. Geophys. Res., 76, 7888-7915, 1971.

Sclater, J.G., and R.L. Fisher, Evolution of the East Central Indian Ocean with emphasis on the tectonic setting of the Ninetyeast Ridge, Bull. Geol. Soc. Amer., 85, 683-702, 1974.

Sclater, J.G., R. Jarrard, B. McGowran, and S. Gartner, A comparison of the magnetic and biostratigraphic time scales, in: von der Borch, C.C., Sclater, J.G., et al., Initial reports of the Deep Sea Drilling Project, vol. 22: Washington, D.C., U.S. Govt. Printing Office, 1974.

Sengupta, M.K., The structure of the earth's mantle from body wave observations, PhD Thesis, pp.541, Mass. Inst. Tech., Cambridge, 1975.

Simmons, G. and H. Wang, Single crystal constants and calculated aggregate properties: A handbook, MIT Press, Cambridge, Mass., 1971.

Sipkin, S.A., and T.H. Jordan, Lateral heterogeneity of the upper mantle determined from the travel times of Scs, J. Geophys. Res., 80, 1474-1484, 1975.

Sipkin, S.A., and T.H. Jordan, Lateral heterogeneity of the upper mantle determined from the travel times of multiple ScS, J. Geophys. Res, In press, 1976.

Sleep, N.H., Segregation of magma from a mostly crystalline mush, Bull Geol. Soc. Amer, 85, 1225-1232, 1974.

Solomon, S.C., Shear wave attenuation and melting beneath the Mid-Atlantic Ridge, J. Geophys. Res., 78, 6044-6059, 1973.

Solomon, S.C., and B.R. Julian, Seismic constraints on ocean-ridge mantle structure: Anomalous fault-plane solutions from first motions, Geophys. J. Roy. Astr. Soc., 38, 265-285, 1974.

Solomon, S.C., N.H. Sleep, and R.M. Richardson, On the forces driving plate tectonics: Inferences from absolute plate velocities and intraplate stress, Geophys. J. Roy. Astr. Soc., 42, 769-801, 1975.

Sykes, L.R., Mechanisms of earthquakes and nature of faulting along the mid-ocean ridges, J. Geophys. Res., 75, 5729-5743, 1967.

Sykes, L.R., Focal mechanism solutions for earthquakes along the world rift systems, Seismol. Soc. Amer. Bull., 60, 1749-1752, 1970.

Sykes, L.R., and M.L. Sbar, Intraplate earthquakes, lithospheric stresses, and the driving mechanism of plate tectonics, Nature, 245, 298-302, 1973.

Weidner, D.J., and K. Aki, Focal depth and mechanism of mid-ocean ridge earthquakes, J. Geophys. Res., 78, 1818-1831, 1973.

Wyllie, P.J., Role of water in magma generation and ation of diapiric uprise in the mantle, J. Geophys. Res., 76, 1328-1338, 1971a.

Wyllie, P.J., The dynamic earth, J. Wiley and Sons, N.Y., 1975b.

TABLE CAPTIONS

Table 1) Parameters of the 25 earthquakes studied. Source of the hypocentral data: ISC

Table 2) Comparison of local shear velocities in the spreading lithosphere, within age-depth blocks, measured by Forsyth (1976) using surface wave inversion, with those modelled in the present study for a gabbro-eclogite, and a peridotite, upper mantle. All values in km/sec.

Table 3) Depths for events 2, 3, 6, 8, and 13, calculated 1) using a least squares method on the P arrivals (ISC), 2) using surface wave analysis (Weidner and Aki, 1973), and 3) using depth phases (present study). All values in km.

Table 4) Extension of Bullen's (1937) ellipticity corrections for S wave travel times, for latitudes greater than 60°. Corrections should be subtracted from travel times. All values in seconds.

Table 1

Event Number	Date	Ocean	Lat.	Long.	Origin Time	Mag.	Depth	Age	Ref. on Age	Type	Ref. on Type
1	Sept.20,1969	Atlantic	58.35N	32.08W	05:08:57.8	5.6	33	0±2	7	N	11
2	Nov. 16 1965	Atlantic	31.00N	41.53W	15:24:44.0	5.9	21±16	0±2	7	N	2
3	June 2,1965	Atlantic	15.93N	46.69W	23:40:23.1	5.8	27±2	0±2	7	N	3
4	Sept.17,1964	Atlantic	44.58N	31.34W	15:02:01.5	5.5	24	20±2	7	T	1
5	Sept. 3,1968	Atlantic	20.58N	62.30W	15:37:00.3	5.6	34±2	97±5	7	T	1
6	Oct. 23,1964	Atlantic	19.80N	56.11W	01:56:05.6	6.2	43±9	71±3	7	T-SS	1
7	Oct. 20,1972	Atlantic	20.60N	29.69W	04:33:49.9	5.7	39±5	95±4	7	SS	4
8	Sept.30,1971	Atlantic	00.45S	04.89W	21:24:10.8	6.0	30±4	47±10	10	T	1
9	Mar. 31,1970	Indian	03.78S	69.70E	18:18:28.0	5.5	59±17	10±2	8	N	1
10	Mar. 2,1968	Indian	06.09S	71.41E	22:02:24.2	5.5	28±1	17±3	8	N	1
11	Sept.12,1965	Indian	06.46S	70.76E	22:02:37.7	6.1	62±13	14±3	8	N	1
12	Dec. 3,1964	Indian	14.84S	66.76E	03:50:01.7	5.7	50±21	2±2	8	N	5
13	Oct. 10,1970	Indian	03.56S	86.19E	08:53:04.5	5.8	32±2	75±5	9	SS	1
14	May 25,1964	Indian	09.08S	88.89E	19:44:05.9	5.7	25±22	56±3	9	SS	1
15	June 26,1971	Indian	05.18S	96.90E	19:27:11.0	5.9	0±17	56±2	9	T	1
16	Feb. 17,1966	Indian	32.20S	78.93E	11:47:57.3	6.0	7	3±1.5	8	N	5
17	Dec. 19,1965	Indian	32.24S	78.87E	22:06:33.0	5.5	33	3±1.5	8	N	5
18	Oct. 8,1968	Indian	39.85S	87.74E	07:43:22.8	5.8	33	10±1	8	N	1

Table 1 cont'

Event Number	Date	Ocean	Lat.	Long.	Origin Time	Mag.	Depth	Age	Ref. on Age	Type	Ref. on Type
19	Jan. 21,1970	Pacific	07.03N	104.24W	17:51:37.4	6.1	23±2	35±1	10	N	6
20	May 2,1972	Pacific	05.22N	100.32W	06:56:23.2	5.9	30±5	4±1	10	N	6
21	Jan. 29,1969	Pacific	17.15S	171.57W	17:44:31.6	6.0	35±2	>100	10	T	1
22	Nov. 12,1967	Pacific	17.19S	171.98W	10:36:51.0	5.6	28±12	>100	10	T	1
23	May 9,1971	Pacific	39.78S	104.87W	08:25:01.1	6.0	29±2	10±1	10	T	1
24	Aug. 25,1964	Arctic	78.15N	126.65E	13:47:19.3	6.2	34±3	0±2		N	2
25	Feb. 13,1967	Atlantic	52.82N	34.25W	23:14:22.3	5.6	17±1	NA	7	SS	

References: 1) Sykes and Sbar,1973
2) Sykes,1967
3) Sykes,1970
4) R.M.Richardson (pers. comm.)
5) Banghar and Sykes,1969
6) Anderson et al.,1974
7) Pitman and Talwani,1972
8) McKenzie and Sclater,1971
9) Sclater and Fisher,1974
10) Pitman et al.,1974
11) Solomon and Julian,1974

Table 2

	Forsyth (1976)	Present Study	
		Peridotite	Gabbro
10-20 my 20-45 km	4.43±.03	4.34	3.89
20-40 my 20-45 km	4.46±.04	4.52	4.24
20-40 my 40-70 km	4.43±.04	4.40	4.08
20-40 my 80-140 km	4.10±.04	4.10	4.00
100-140 my 25-50 km	4.66±.025	4.67	4.58
100-140 my 55-90 km	4.49±.04	4.48	4.31
100-140 my 90-150 km	4.25±.04	4.10	4.00

Table 3

EVENT	DEPTH 1*	2**	3**
2	21±16	3	4
3	27±2	3	2
6	43±9		3
8	30±4		1.5
13	32±2		3

Sources: 1) International Seismological Center

2) Weidner and Aki, 1973

3) Present study

* kilometers below sea level

** kilometers below the ocean floor

Table 4

For Latitude 70°

Azimuth	000°	030°	060°	090°	120°	150°	180°
Distance							
30°				-0.9	-0.8	-0.7	-0.7
40°			-1.2	-1.0	-0.8	-0.7	-0.7
50°	-1.4	-1.3	-1.1	-0.8	-0.6	-0.6	-0.6
60°	-1.1	-1.0	-0.8	-0.6	-0.5	-0.4	-0.5
70°	-1.1	-0.9	-0.7	-0.5	-0.5	-0.5	-0.7

For Latitude 80°

Azimuth	000°	030°	060°	090°	120°	150°	180°
Distance							
30°				-1.2	-1.1	-1.0	-1.1
40°	-1.4	-1.3	-1.2	-1.1	-1.0	-1.0	-1.0
50°	-1.3	-1.2	-1.1	-1.0	-0.9	-0.8	-0.9
60°	-1.0	-0.9	-0.8	-0.7	-0.7	-0.6	-0.7
70°	-1.4	-0.9	-0.8	-0.7	-0.7	-0.7	-0.8

For Latitude 90°

Azimuth	All azimuths
Distance	
30°	-1.3
40°	-1.2
50°	-1.1
60°	-0.9
70°	-0.9

FIGURE CAPTIONS

Figure 1) Location of events studied.

Figure 2) Typical shear waves, from long period WWSSN records, subjectively rated 1 (most precise) to 4 (least precise).

Figure 3) Histograms of shear wave travel time residuals from event 20, plotted before and after application of corrections for near station effects and ellipticity of the earth.

Figure 4) Histograms of corrected shear wave travel time residuals from events 1 through 24. Arrows indicate representative residual value, chosen subjectively given quality, quantity, and distribution of the data.

Figure 5) Residuals for 6 events in the Atlantic Ocean plotted against $\sqrt{\text{age}}$ of the lithosphere in which they occurred. Error bars are subjective but indicate proximity of data sets to Gaussian distribution of low variability, and accuracy to which the age of the sea floor is known.

Figure 6) Similar to Figure 5, for 2 events in the Pacific Ocean.

Figure 7) Similar to Figure 5, for 10 events in the Indian Ocean.

Figure 8) Residuals of all events plotted against $\sqrt{age}$. Indian Ocean event residuals are all increased by 2 seconds. A decrease of 6±1 seconds from ridge crest to lithosphere older than 100 m.y. is apparent for all oceans.

Figure 9) Isotherms in the spreading lithosphere calculated after Sleep (1974), and used in the computations.

Figure 10) Velocity models after Solomon and Julian (1974), used in converting peridotite phases to velocity across hydrous and anhydrous solidi.

Figure 11) Phase diagrams used in the computations.

Figure 12) Phase map of the spreading lithosphere, produced by combining the isotherms in Figure 9 with a pressure gradient of .3 kb/km and the wet peridotite phase diagram in Figure 11a.

Figure 13) Shear velocity map of the spreading lithosphere produced by combination of the phase map in Figure 12 with the velocity model in Figure 10 for wet peridotite.

Figure 14) Synthetic residual curves for a dry and a wet gabbro-eclogite upper mantle.

Figure 15) Synthetic residual curves for a dry and a wet peridotite upper mantle.

Figure 16) Residual curve derived from the lithosphere-asthenosphere velocity model of Leeds et al., (1974). Extrapolation to ridge crest is arbitrary.

Figure 17) Short period vertical component WWSSN seismograms from event 2.

Figure 18) Short period vertical component WWSSN seismograms from event 3.

Figure 19) Short period vertical component WWSSN seismograms from event 6.

Figure 20) Short period vertical component WWSSN seismograms from event 8.

Figure 21) Short period vertical component WWSSN seismograms from event 13.

Figure 22) Residual versus azimuth for event 25, on the Gibbs Fracture zone, east of the Mid-Atlantic Ridge.

Figure 23) Residual versus azimuth for event 4, west of the Mid-Atlantic Ridge.

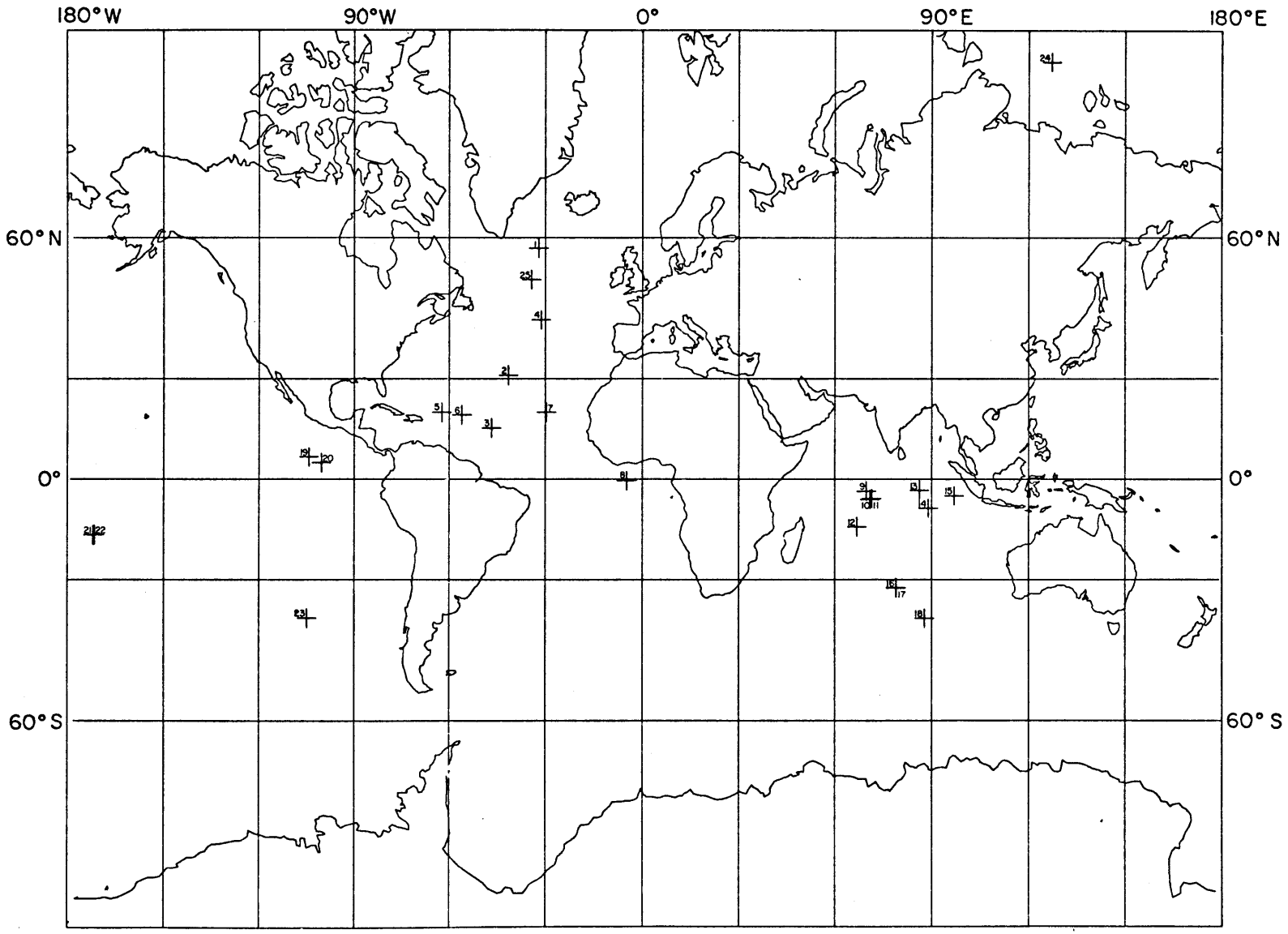

Figure 1.

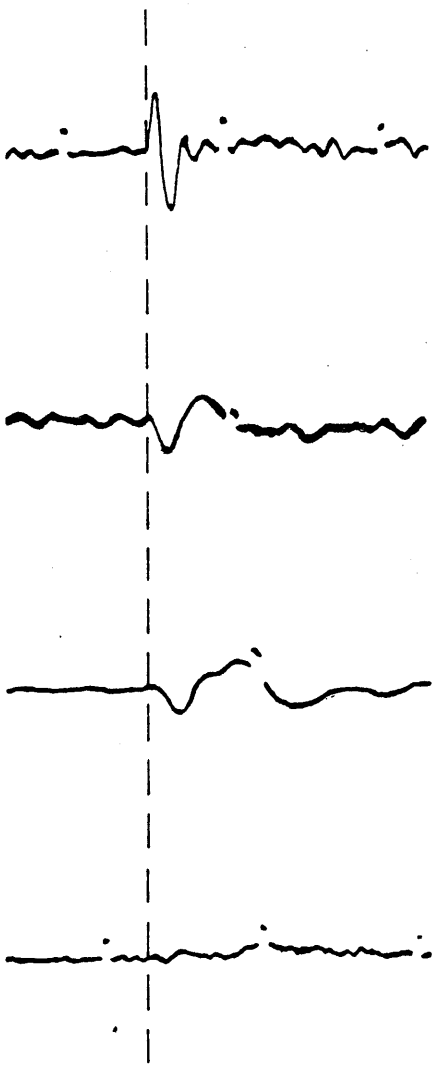

RATING	EVENT	STATION
1	5	TRI (Italy)
2	3	COR (Oregon)
3	3	KON (Norway)
4	5	KTG (Greenland)

Figure 2.

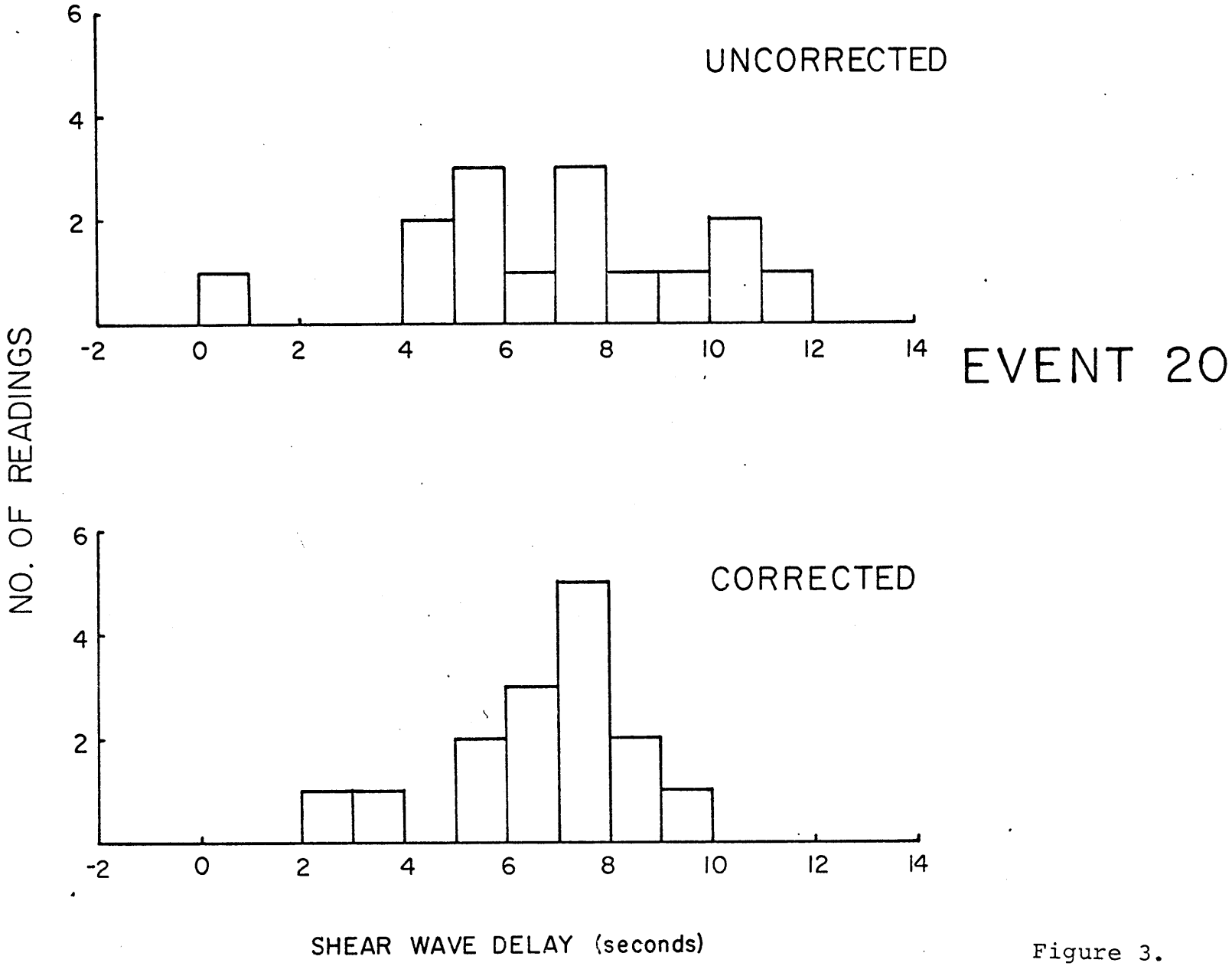
UNCORRECTED
CORRECTED
EVENT 20
NO. OF READINGS
SHEAR WAVE DELAY (seconds)
6
4
2
-2
0
2
4
6
8
10
12
14

Figure 3.

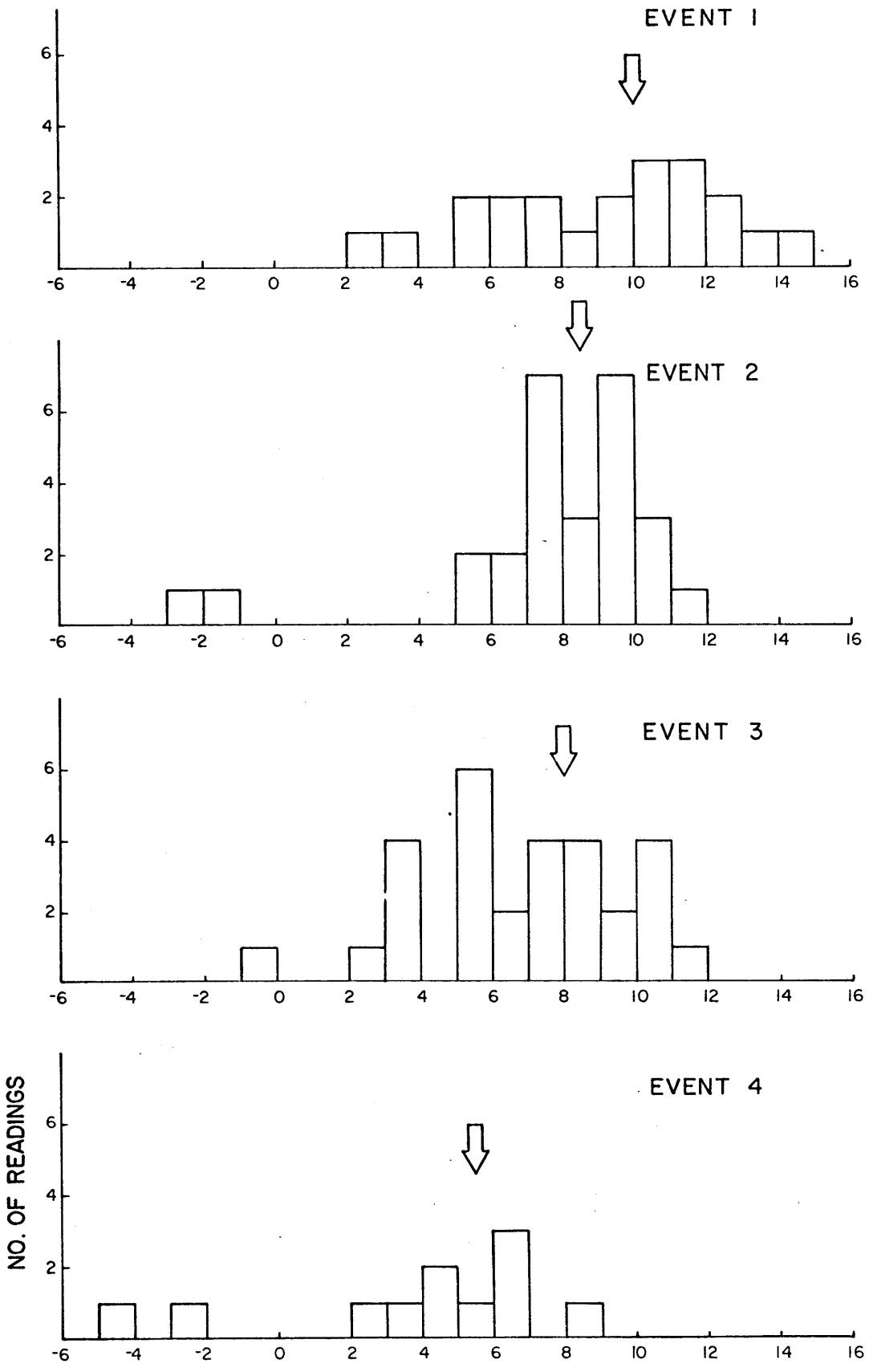
EVENT 1
EVENT 2
EVENT 3
EVENT 4
NO. OF READINGS
SHEAR WAVE DELAY (seconds)

Figure 4.

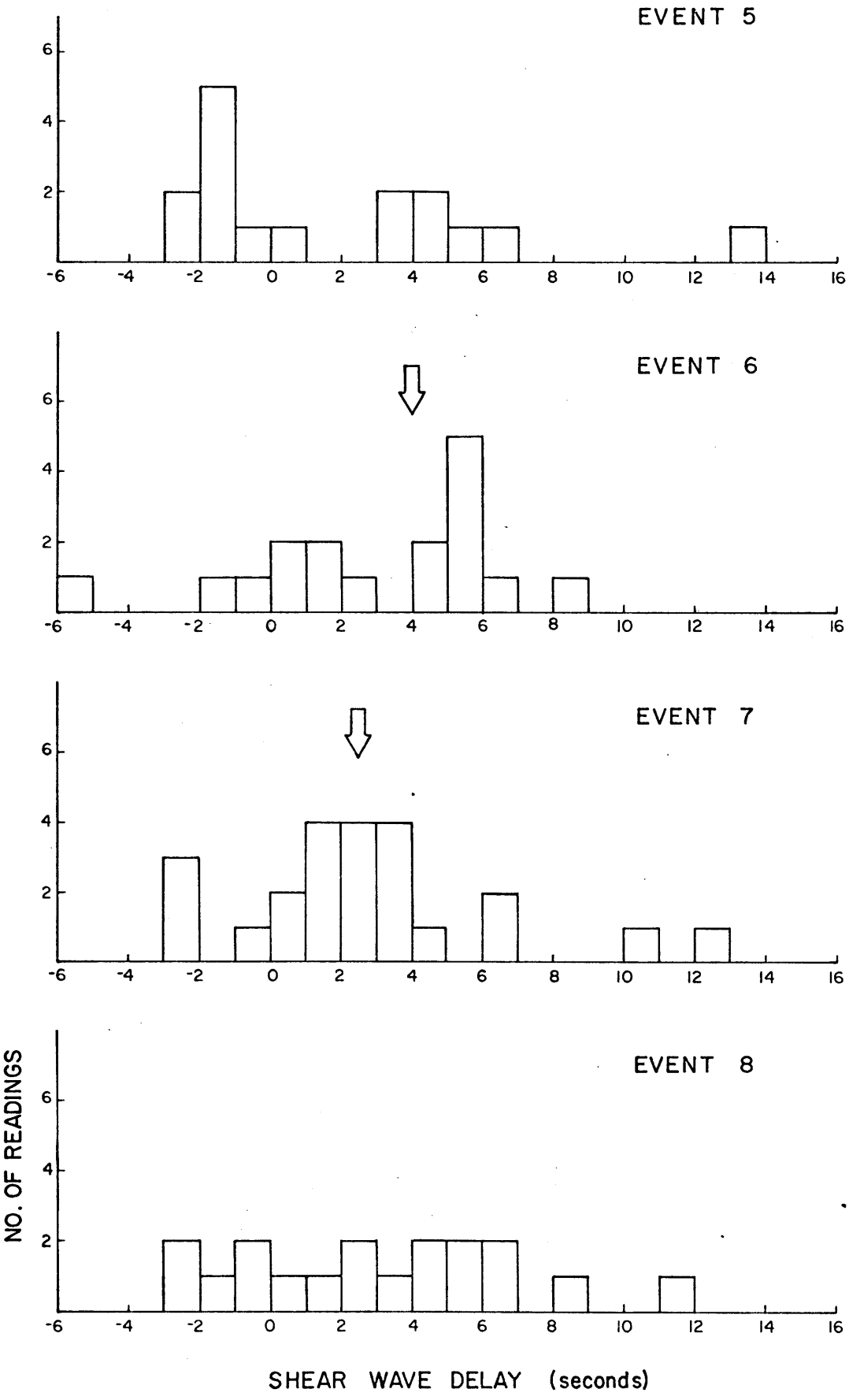
EVENT 5
EVENT 6
EVENT 7
EVENT 8
NO. OF READINGS
SHEAR WAVE DELAY (seconds)
-6 -4 -2 0 2 4 6 8 10 12 14 16
2 4 6

Figure 4.

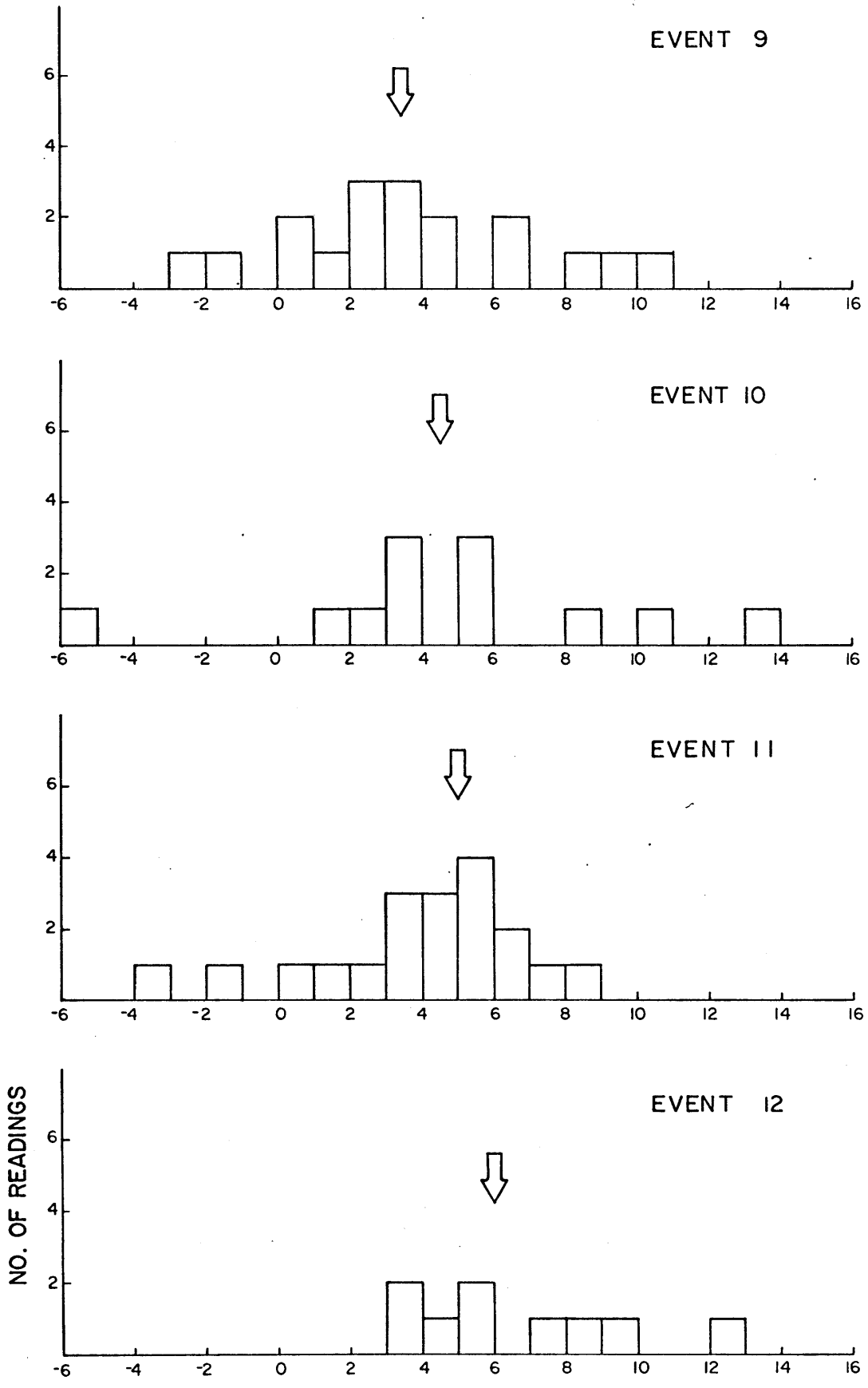
EVENT 9
EVENT 10
EVENT 11
EVENT 12
NO. OF READINGS
SHEAR WAVE DELAY (seconds)
-6 -4 -2 0 2 4 6 8 10 12 14 16
2 4 6

Figure 4.

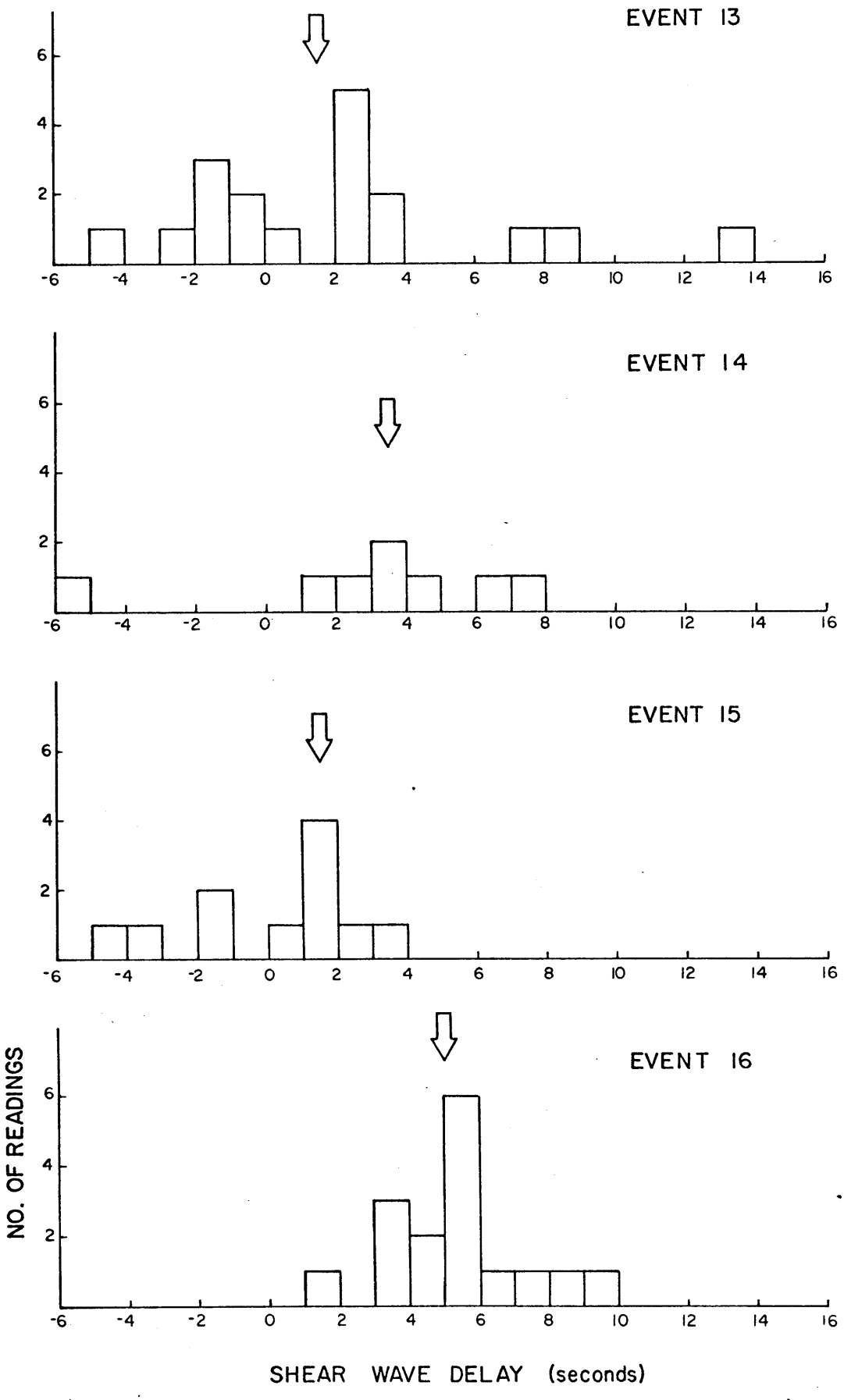
EVENT 13
EVENT 14
EVENT 15
EVENT 16
NO. OF READINGS
SHEAR WAVE DELAY (seconds)

Figure 4.

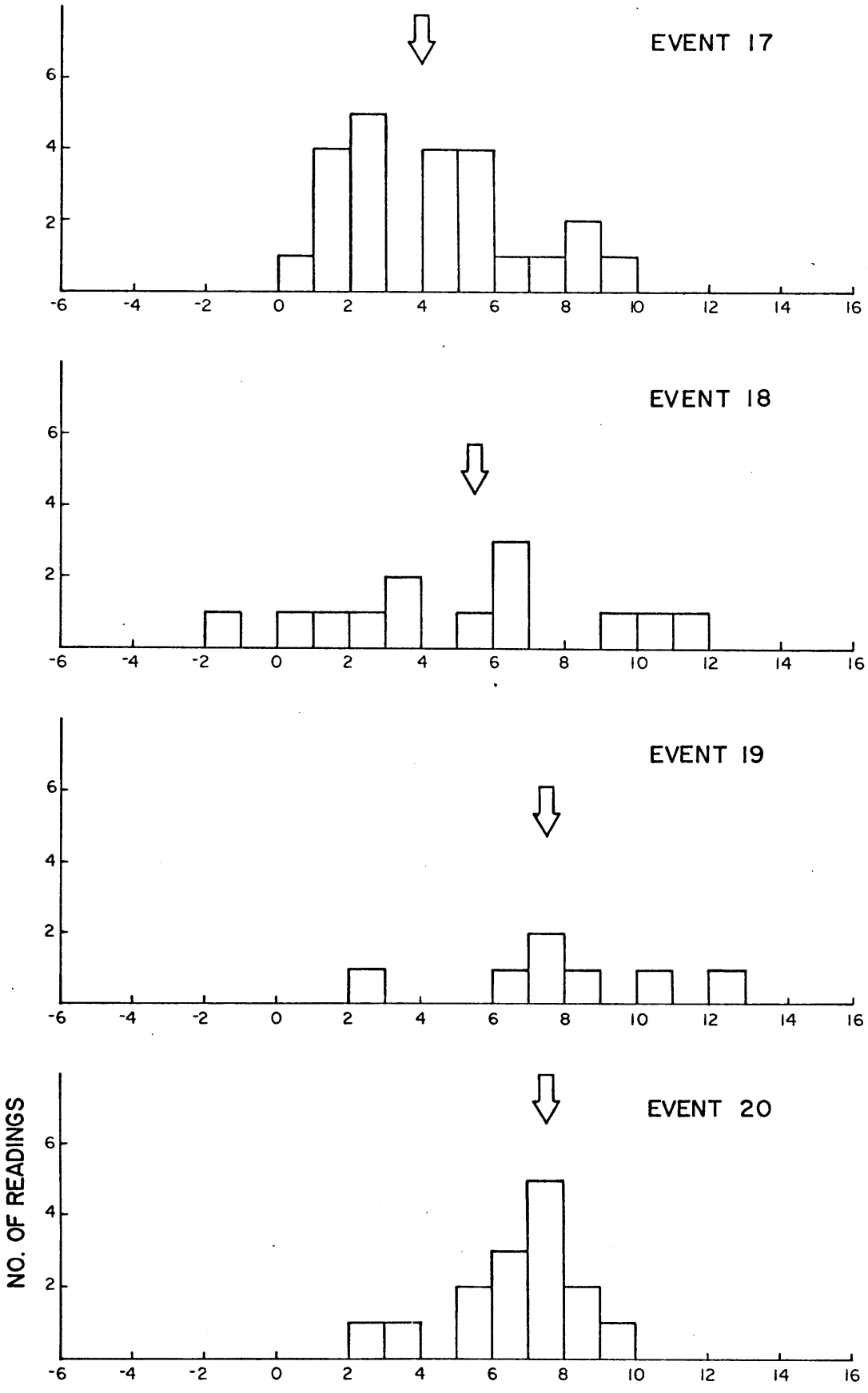
EVENT 17
EVENT 18
EVENT 19
EVENT 20
NO. OF READINGS
SHEAR WAVE DELAY (seconds)
-6 -4 -2 0 2 4 6 8 10 12 14 16
2 4 6

Figure 4.

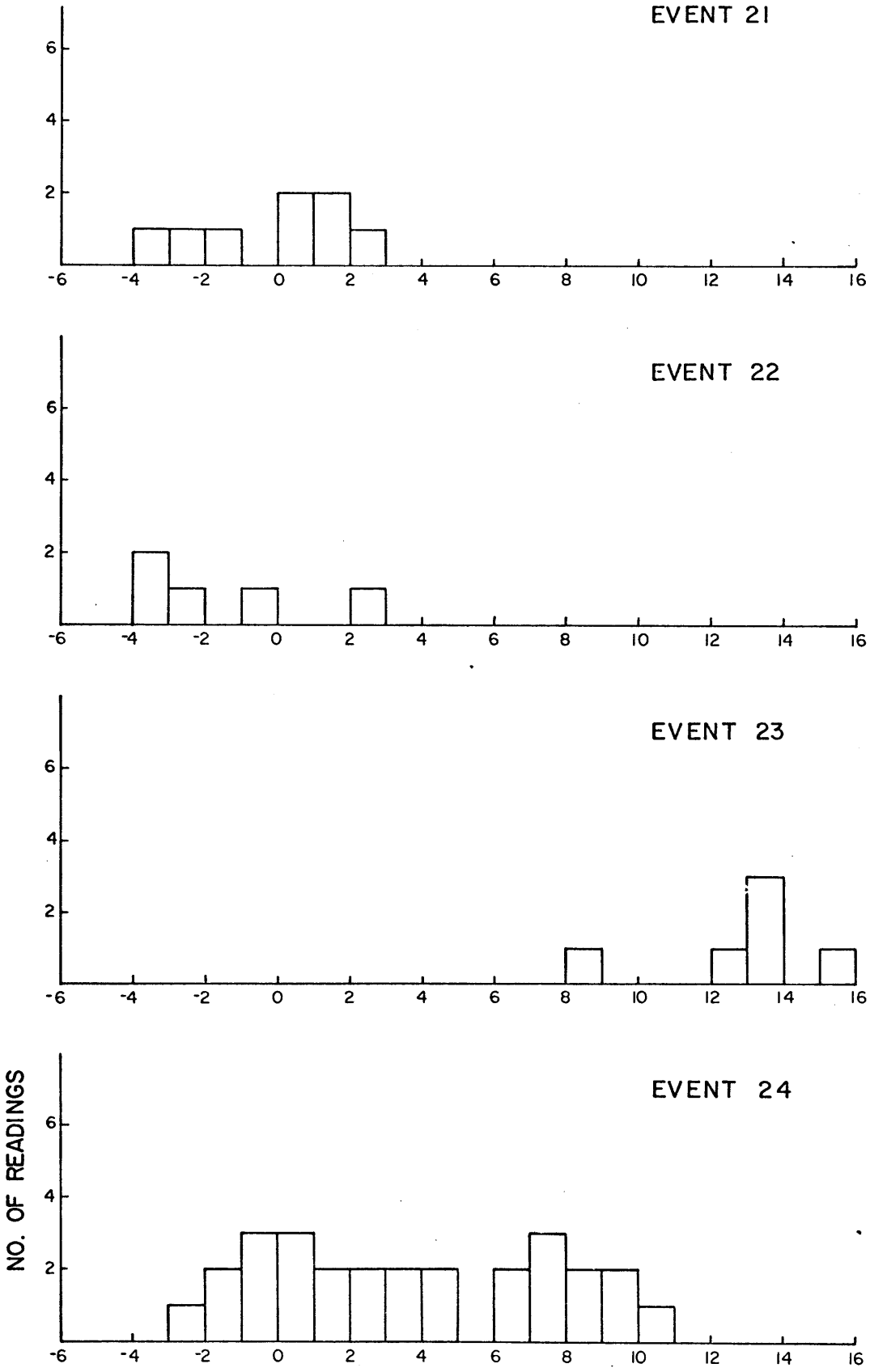
EVENT 21
EVENT 22
EVENT 23
EVENT 24
NO. OF READINGS
SHEAR WAVE DELAY (seconds)
2
4
6
-6
-4
-2
0
2
4
6
8
10
12
14
16

Figure 4.

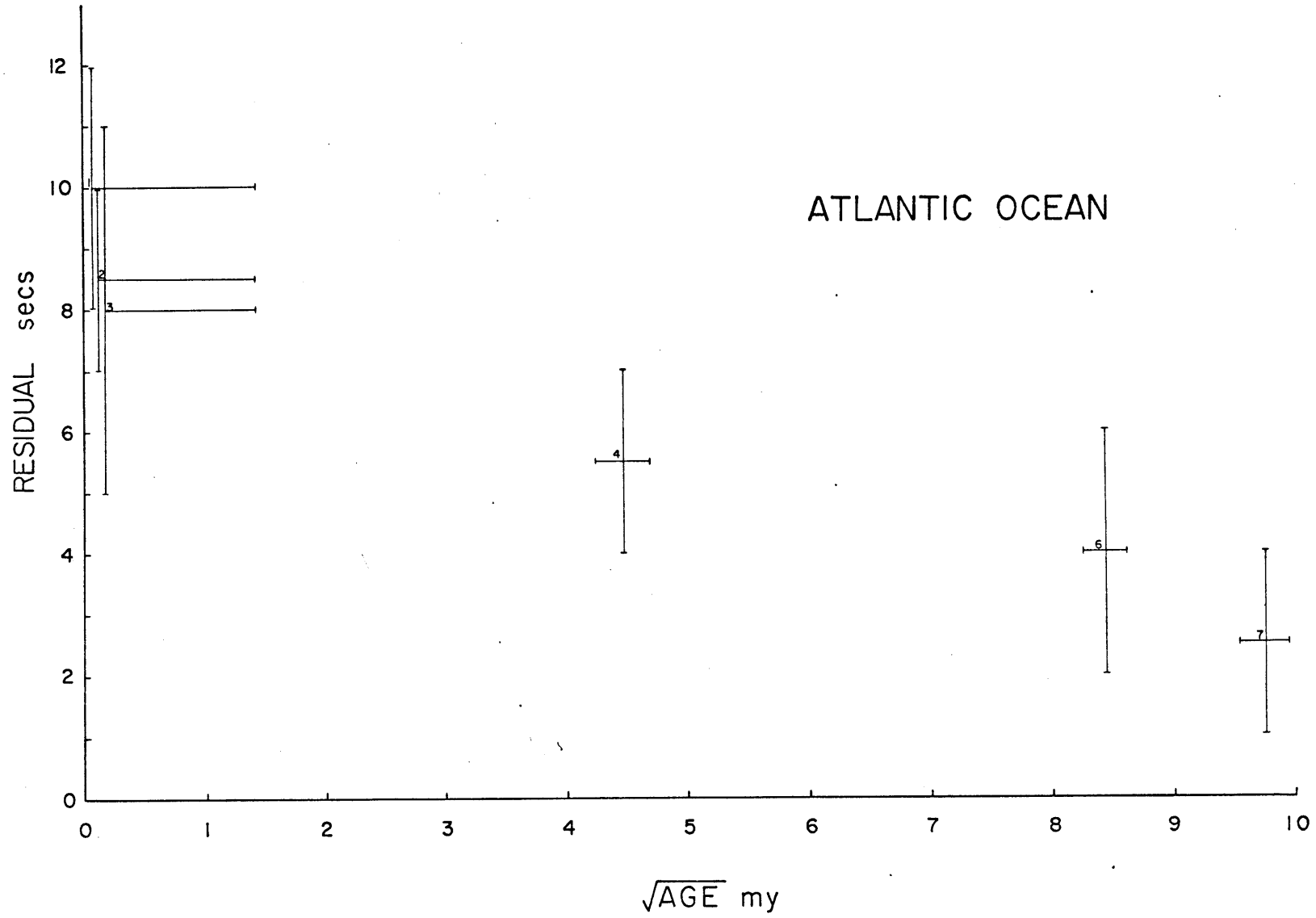
ATLANTIC OCEAN
RESIDUAL secs
√AGE my
0
2
4
6
8
10
12
0
1
2
3
4
5
6
7
8
9
10
1
2
3
4
6
7

Figure 5.

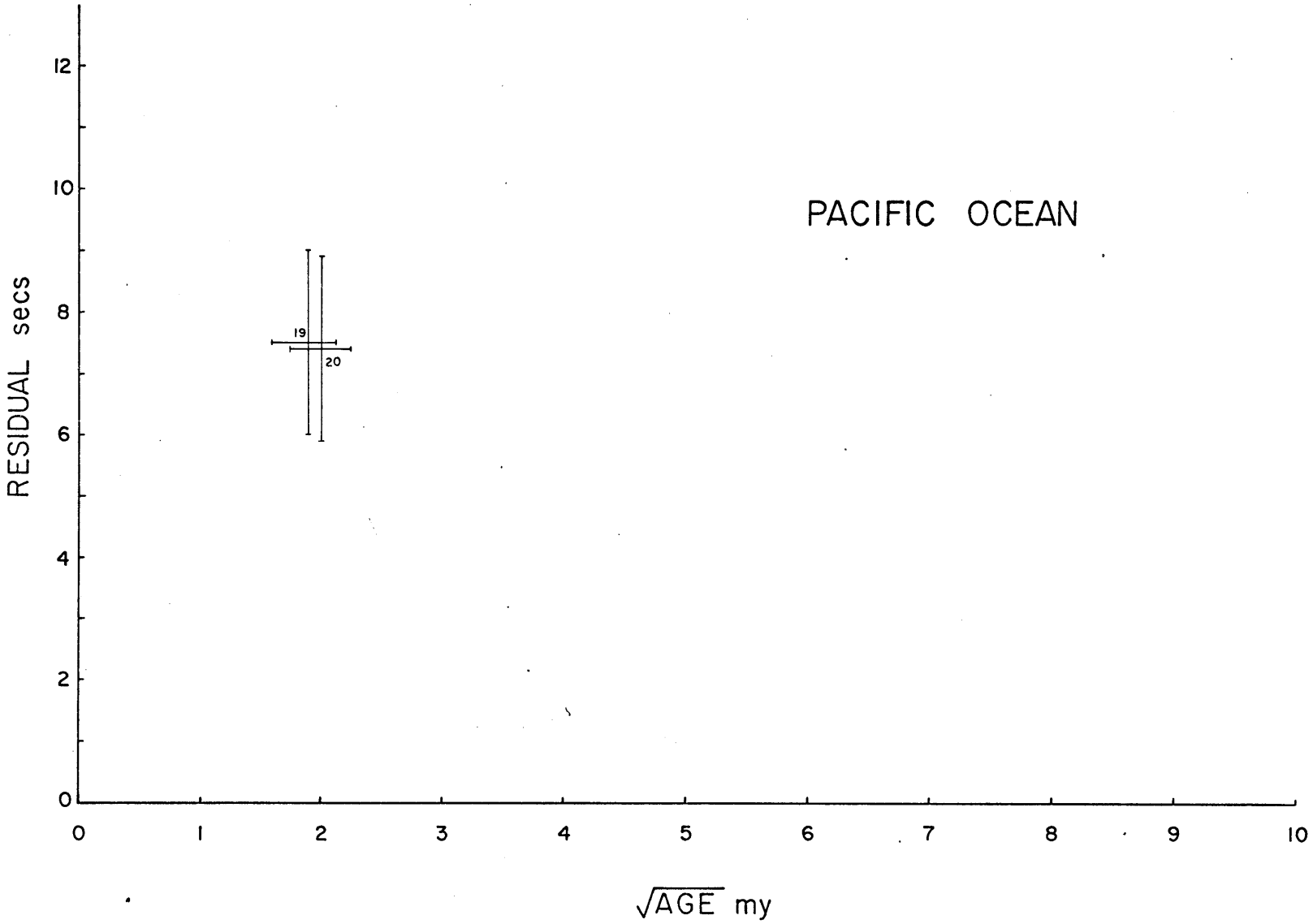
PACIFIC OCEAN
RESIDUAL secs
0
2
4
6
8
10
12
19
20
0
1
2
3
4
5
6
7
8
9
10
√AGE my

Figure 6.

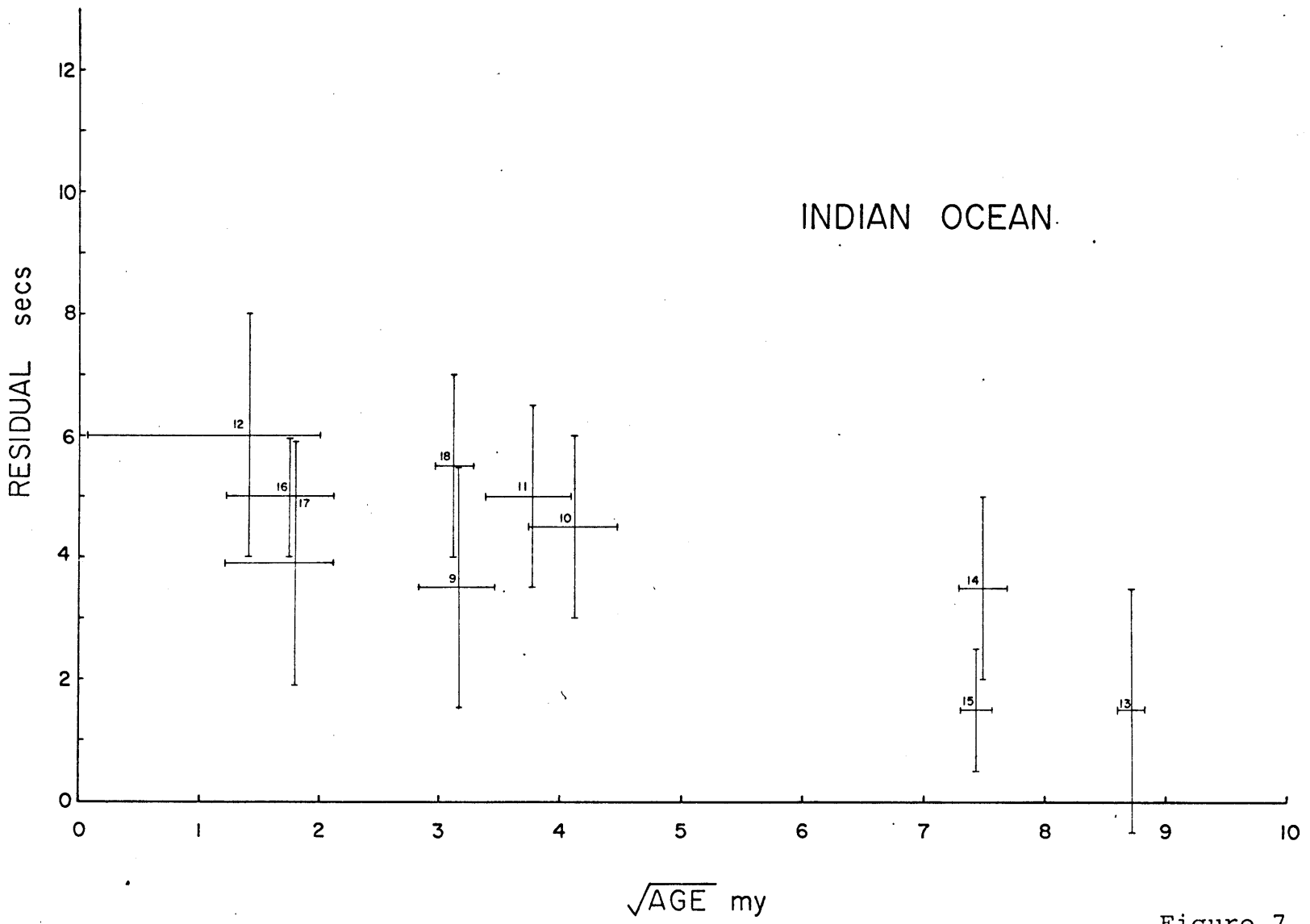
INDIAN OCEAN
RESIDUAL secs
0
2
4
6
8
10
12
0
1
2
3
4
5
6
7
8
9
10
√AGE my
12
16
17
18
9
11
10
14
15
13

Figure 7.

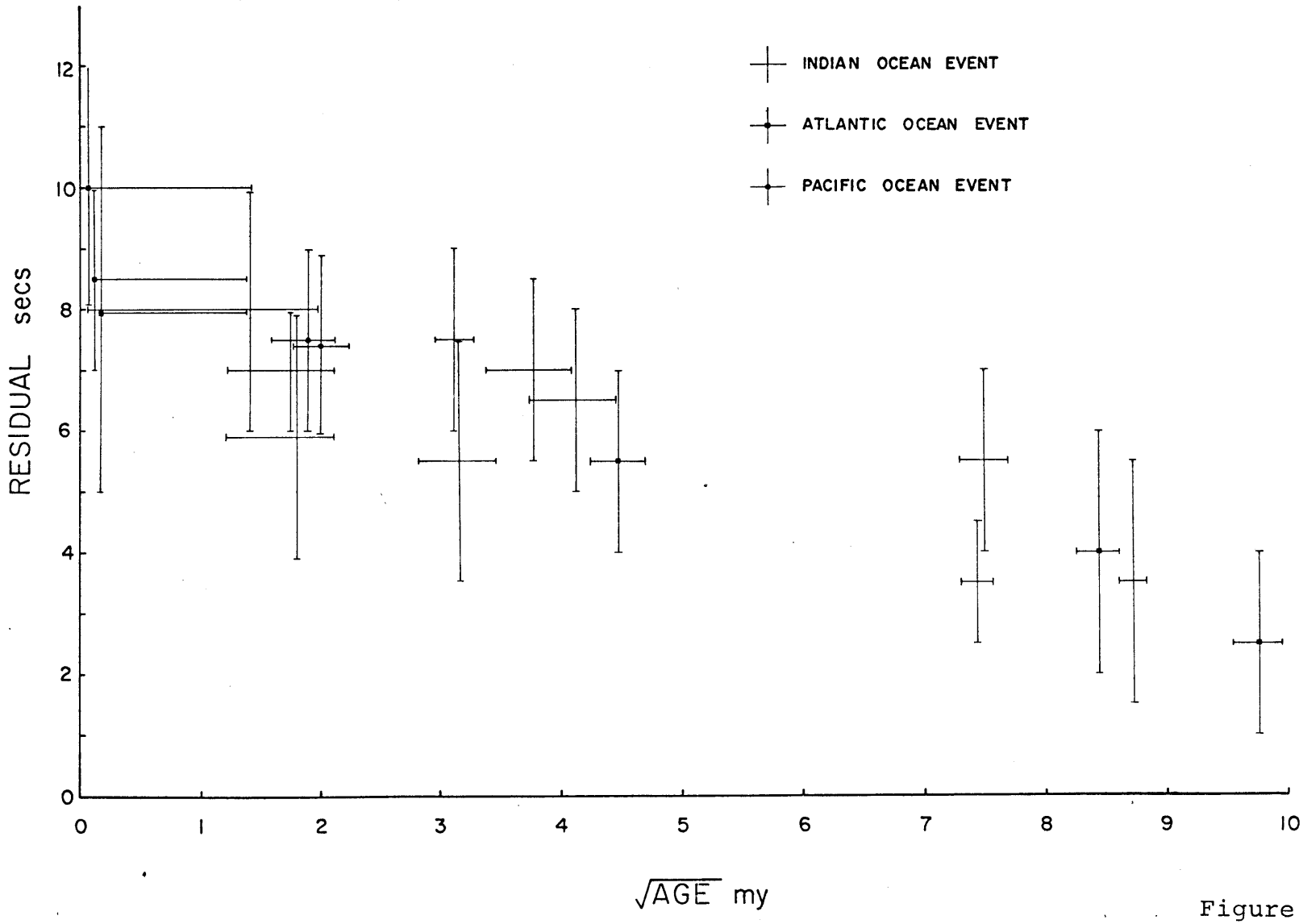
INDIAN OCEAN EVENT
ATLANTIC OCEAN EVENT
PACIFIC OCEAN EVENT
RESIDUAL secs
0
2
4
6
8
10
12
0
1
2
3
4
5
6
7
8
9
10
√AGE my

Figure 8.

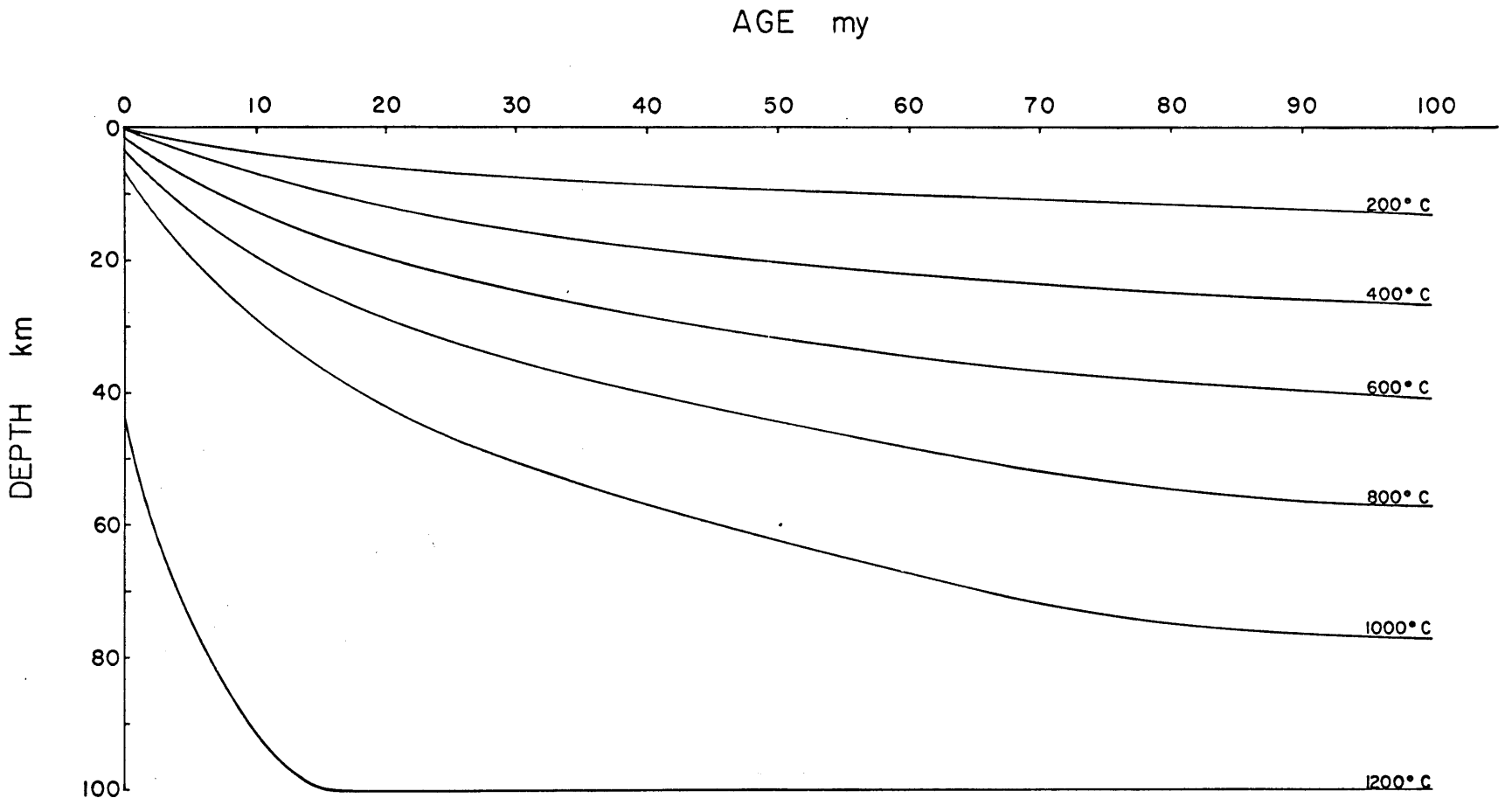
AGE my
0
10
20
30
40
50
60
70
80
90
100
DEPTH km
0
20
40
60
80
100
200° C
400° C
600° C
800° C
1000° C
1200° C

Figure 9.

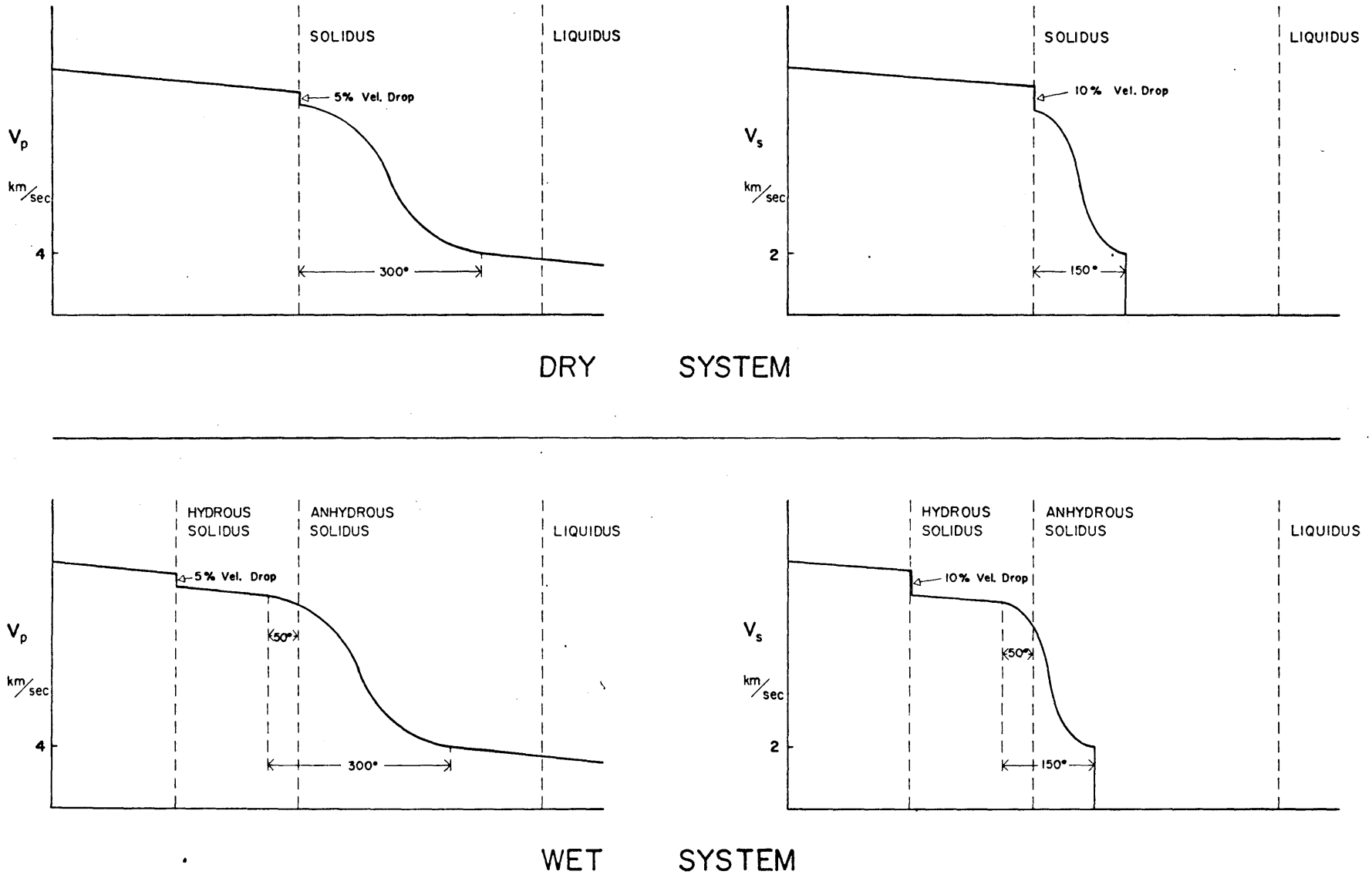
SOLIDUS
LIQUIDUS
5% Vel. Drop
V_p
km/sec
4
300°
SOLIDUS
LIQUIDUS
10% Vel. Drop
V_s
km/sec
2
150°
DRY SYSTEM
HYDROUS SOLIDUS
ANHYDROUS SOLIDUS
LIQUIDUS
5% Vel. Drop
50°
V_p
km/sec
4
300°
HYDROUS SOLIDUS
ANHYDROUS SOLIDUS
LIQUIDUS
10% Vel. Drop
50°
V_s
km/sec
2
150°
WET SYSTEM

Figure 10.

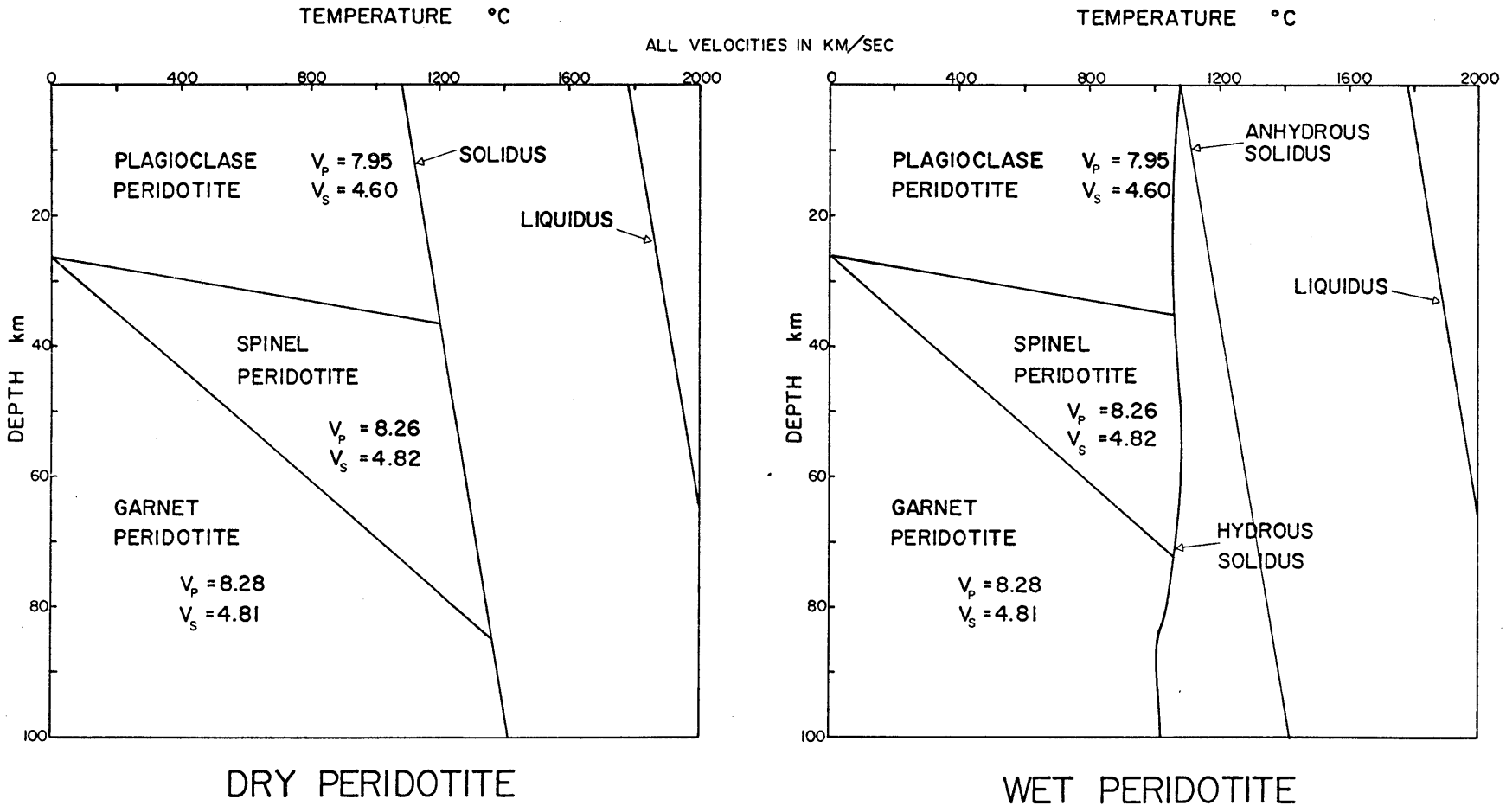
TEMPERATURE °C
ALL VELOCITIES IN KM/SEC
0
400
800
1200
1600
2000
DEPTH km
20
40
60
80
100
PLAGIOCLASE PERIDOTITE
V_P = 7.95
V_S = 4.60
SOLIDUS
LIQUIDUS
SPINEL PERIDOTITE
V_P = 8.26
V_S = 4.82
GARNET PERIDOTITE
V_P = 8.28
V_S = 4.81
DRY PERIDOTITE
TEMPERATURE °C
ANHYDROUS SOLIDUS
HYDROUS SOLIDUS
WET PERIDOTITE

Figure 11a.

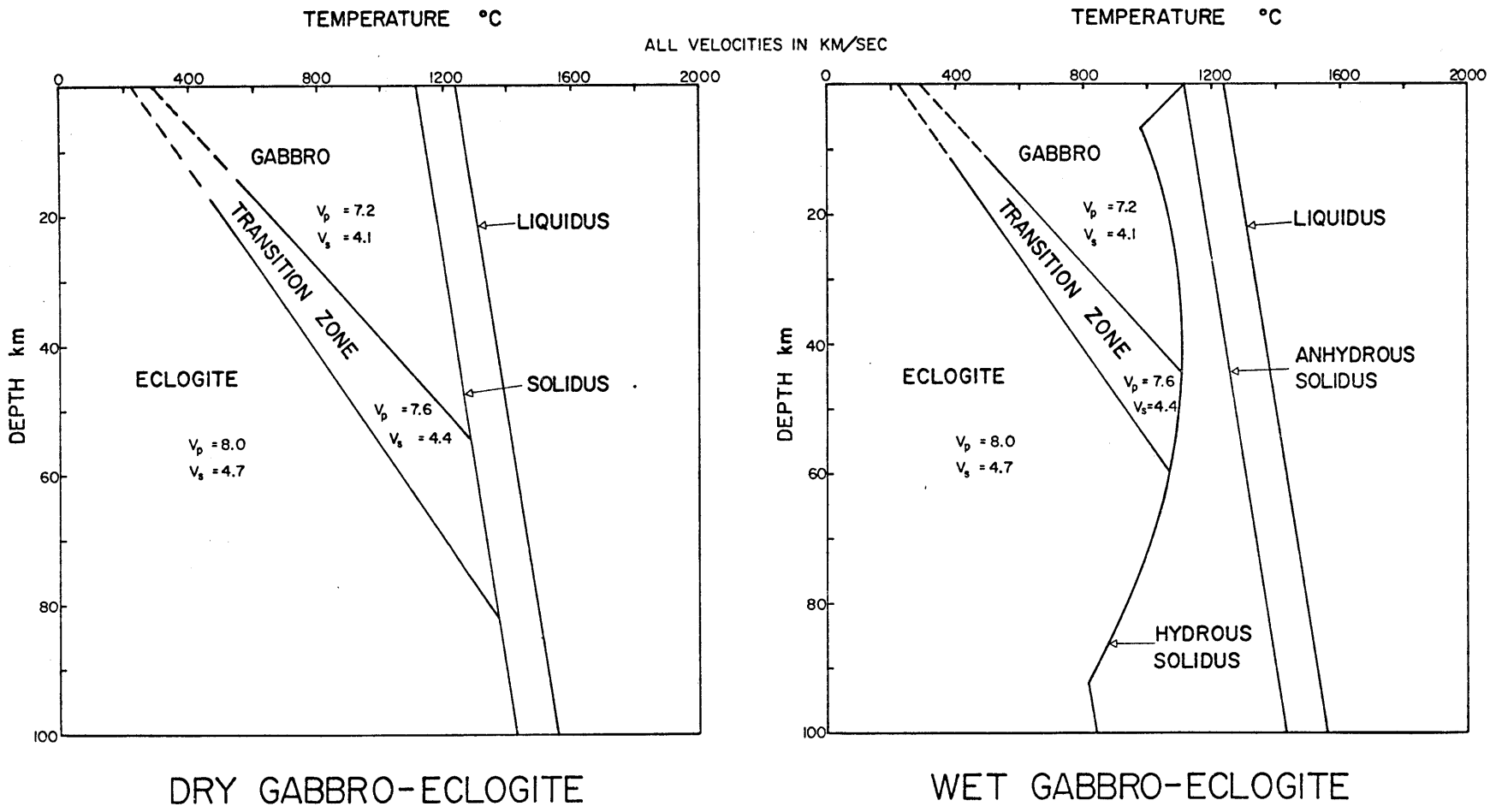
TEMPERATURE °C
ALL VELOCITIES IN KM/SEC
0
400
800
1200
1600
2000
DEPTH km
20
40
60
80
100
GABBRO
V_p = 7.2
V_s = 4.1
TRANSITION ZONE
LIQUIDUS
SOLIDUS
ECLOGITE
V_p = 7.6
V_s = 4.4
V_p = 8.0
V_s = 4.7
DRY GABBRO-ECLOGITE
TEMPERATURE °C
0
400
800
1200
1600
2000
DEPTH km
20
40
60
80
100
GABBRO
V_p = 7.2
V_s = 4.1
TRANSITION ZONE
LIQUIDUS
ANHYDROUS SOLIDUS
ECLOGITE
V_p = 7.6
V_s = 4.4
V_p = 8.0
V_s = 4.7
HYDROUS SOLIDUS
WET GABBRO-ECLOGITE

Figure 11b.

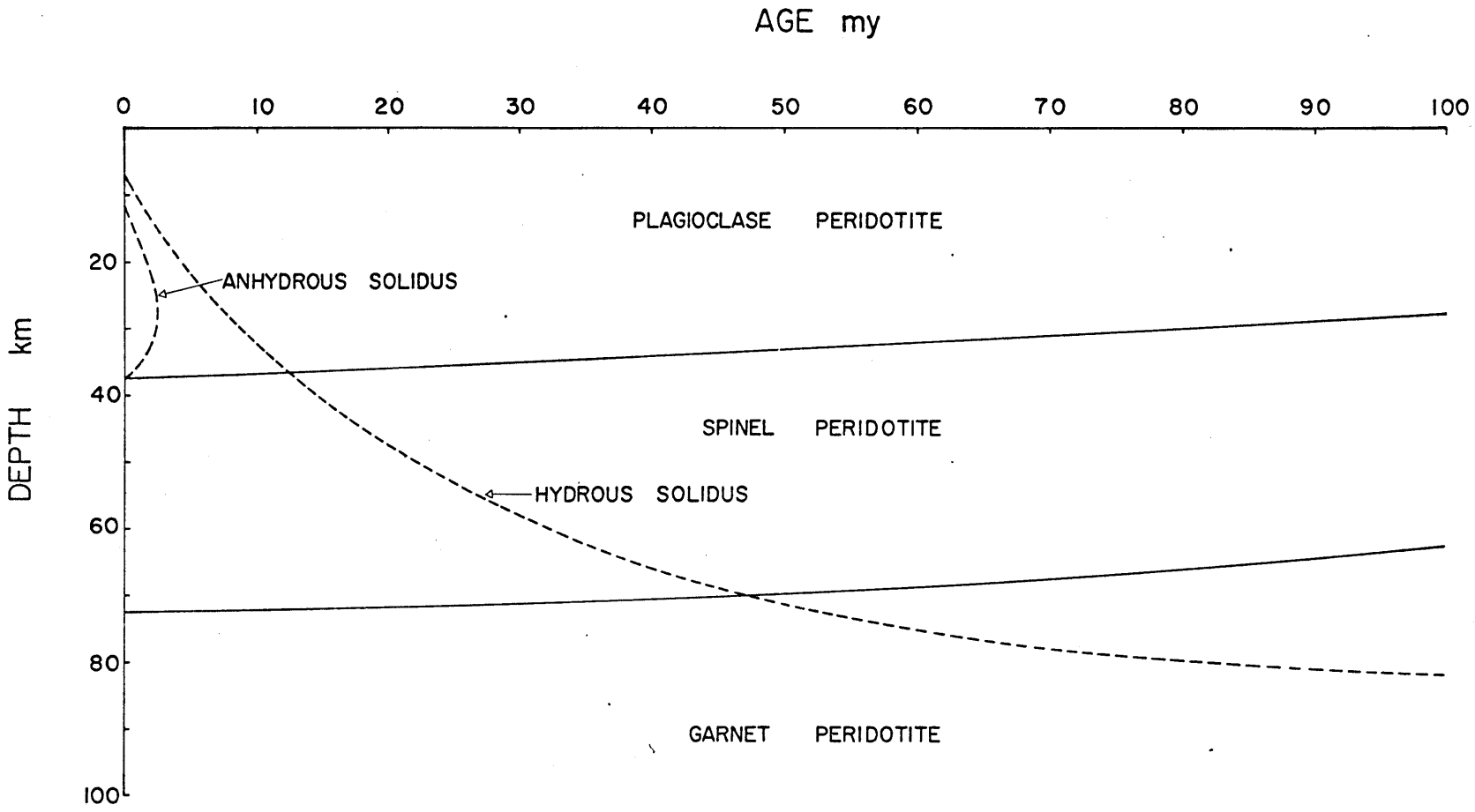
AGE my
0
10
20
30
40
50
60
70
80
90
100
DEPTH km
20
40
60
80
100
PLAGIOCLASE PERIDOTITE
ANHYDROUS SOLIDUS
SPINEL PERIDOTITE
HYDROUS SOLIDUS
GARNET PERIDOTITE

Figure 12.

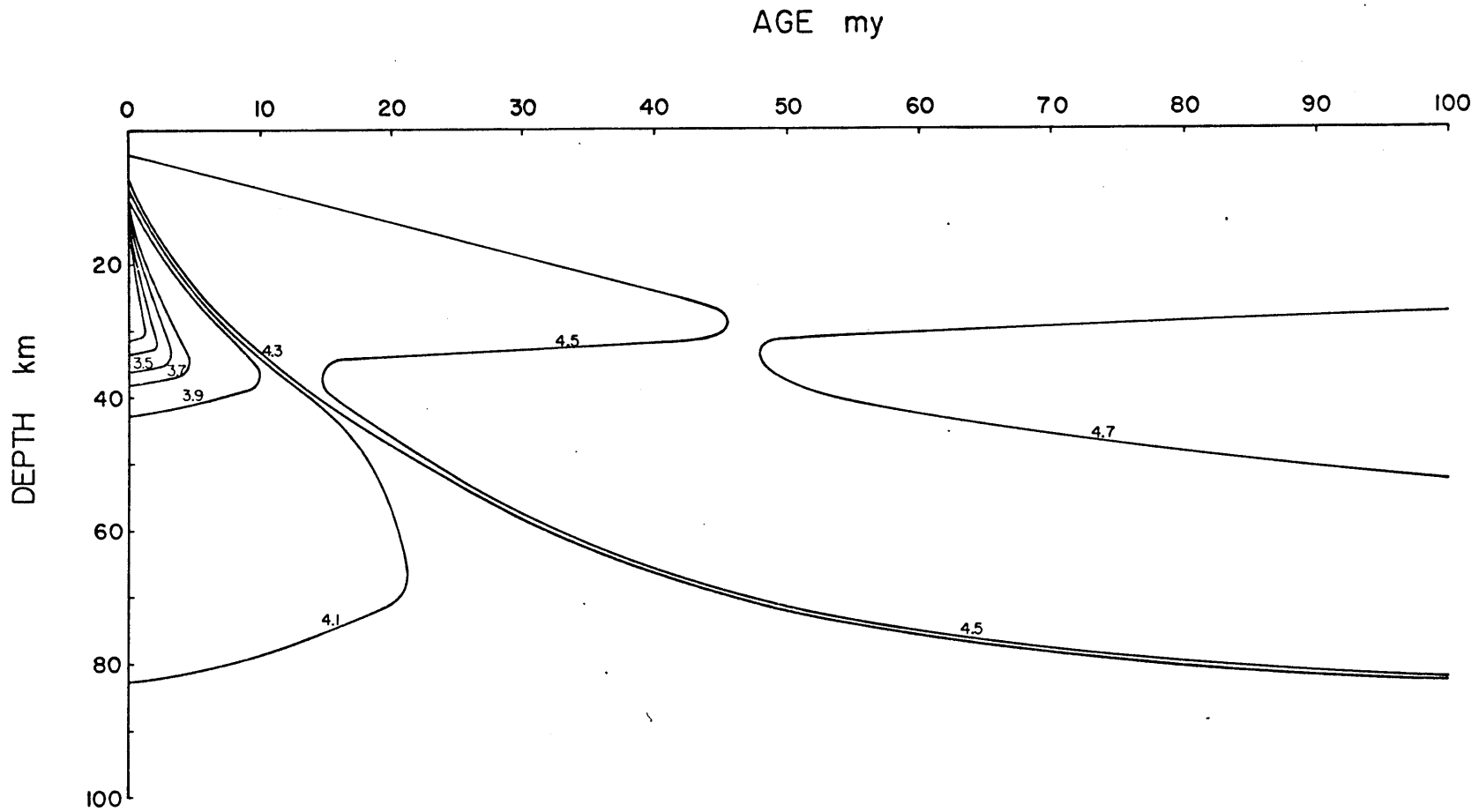
AGE my
0
10
20
30
40
50
60
70
80
90
100
DEPTH km
20
40
60
80
100
3.5
3.7
3.9
4.3
4.5
4.7
4.1
4.5

Figure 13.

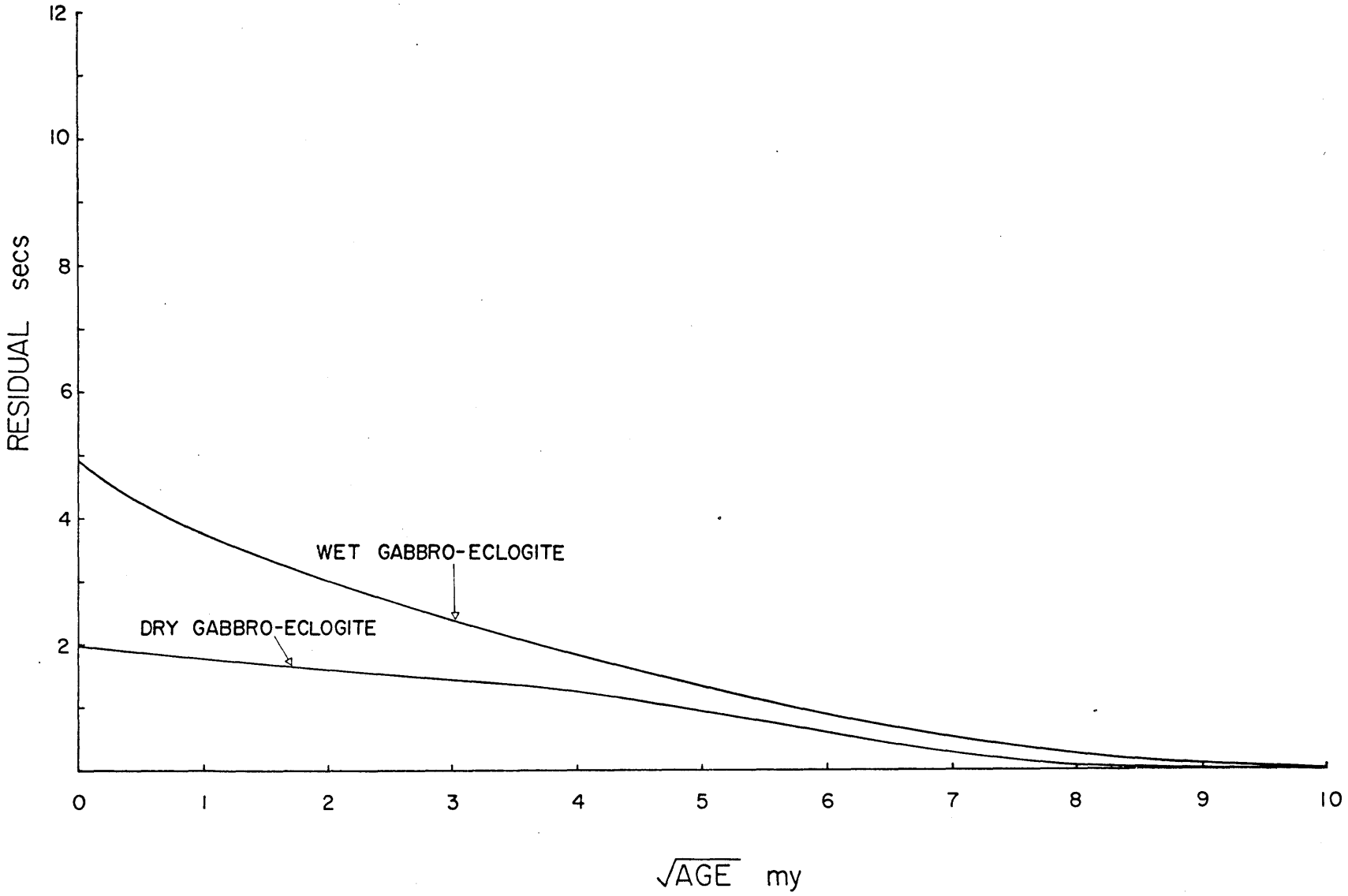
RESIDUAL secs
12
10
8
6
4
2
WET GABBRO-ECLOGITE
DRY GABBRO-ECLOGITE
0
1
2
3
4
5
6
7
8
9
10
√AGE my

Figure 14.

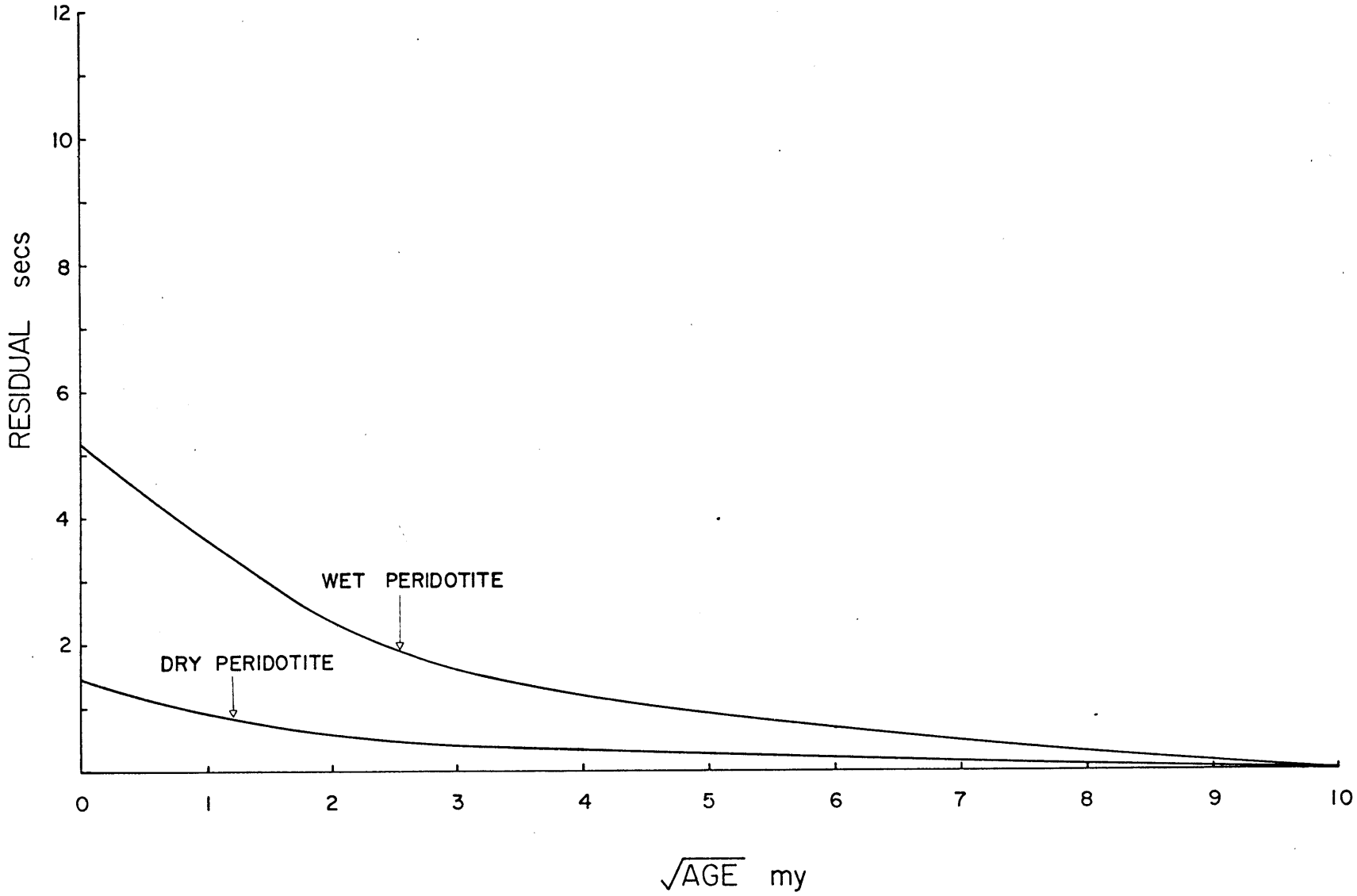
RESIDUAL secs
12
10
8
6
4
2
WET PERIDOTITE
DRY PERIDOTITE
0
1
2
3
4
5
6
7
8
9
10
√AGE my

Figure 15.

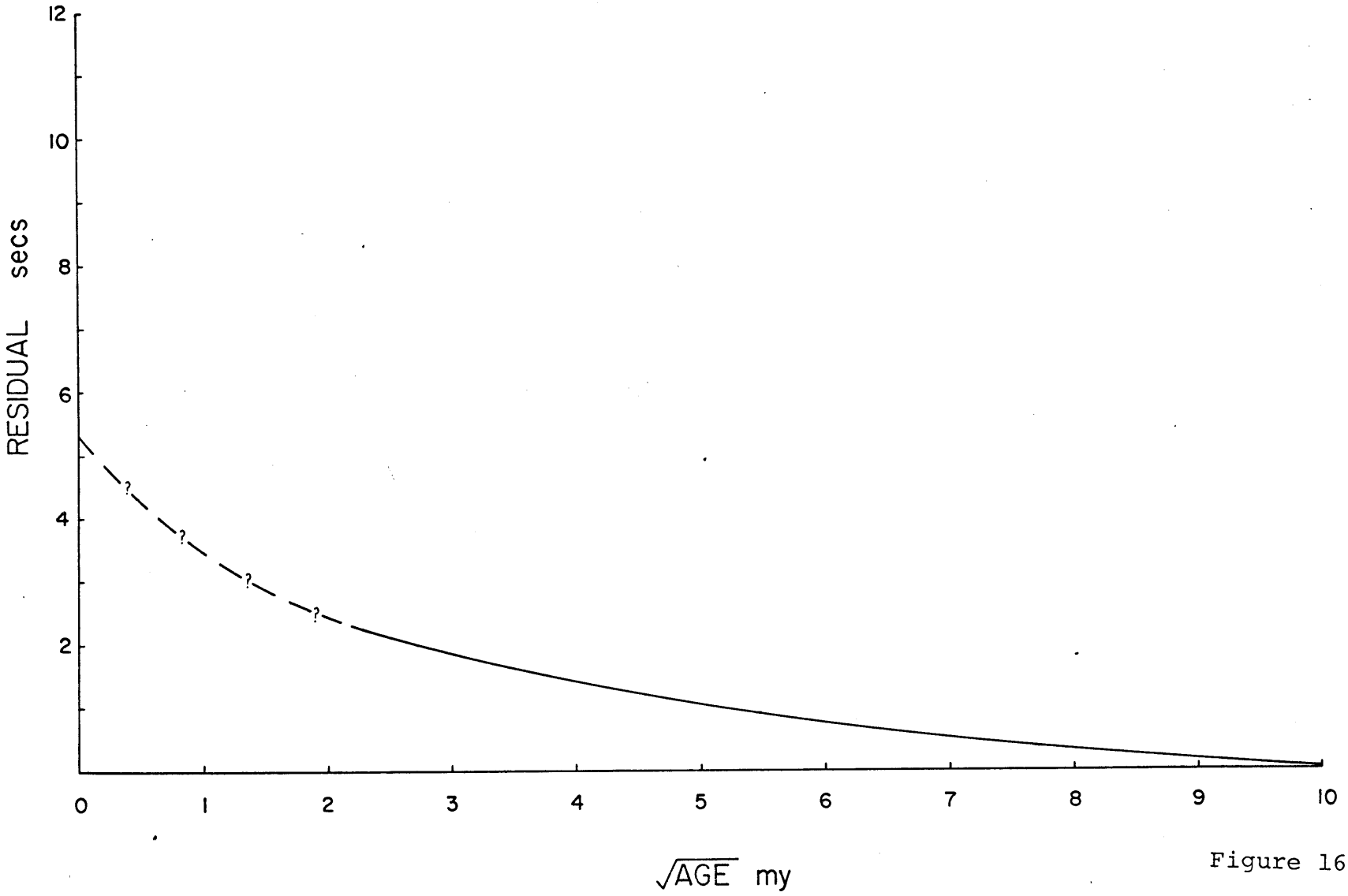

Figure 16.

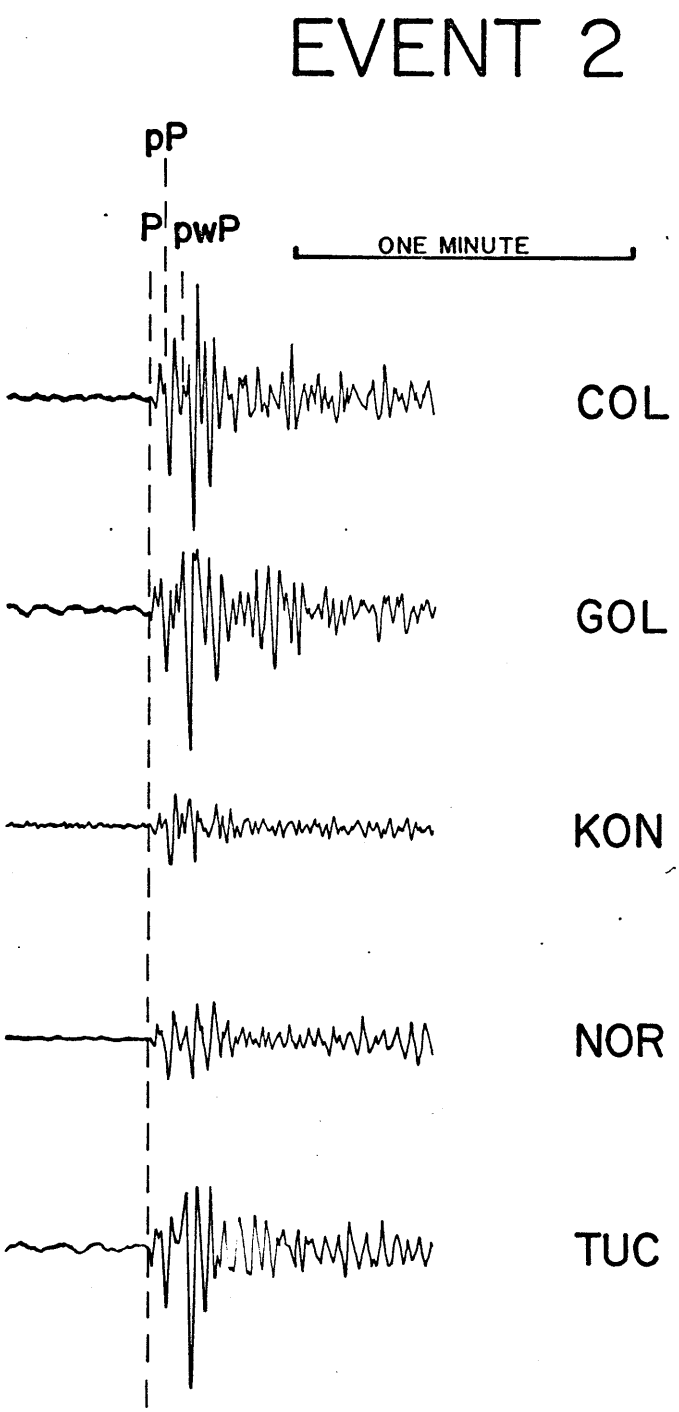

Figure 17.

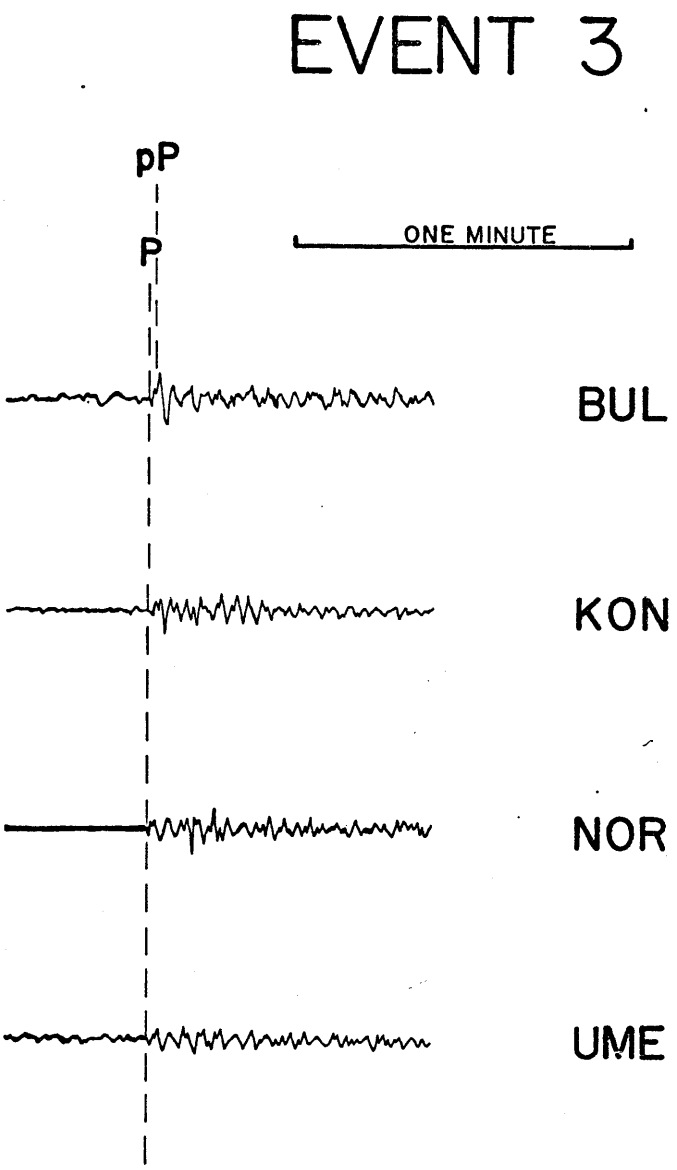

Figure 18.

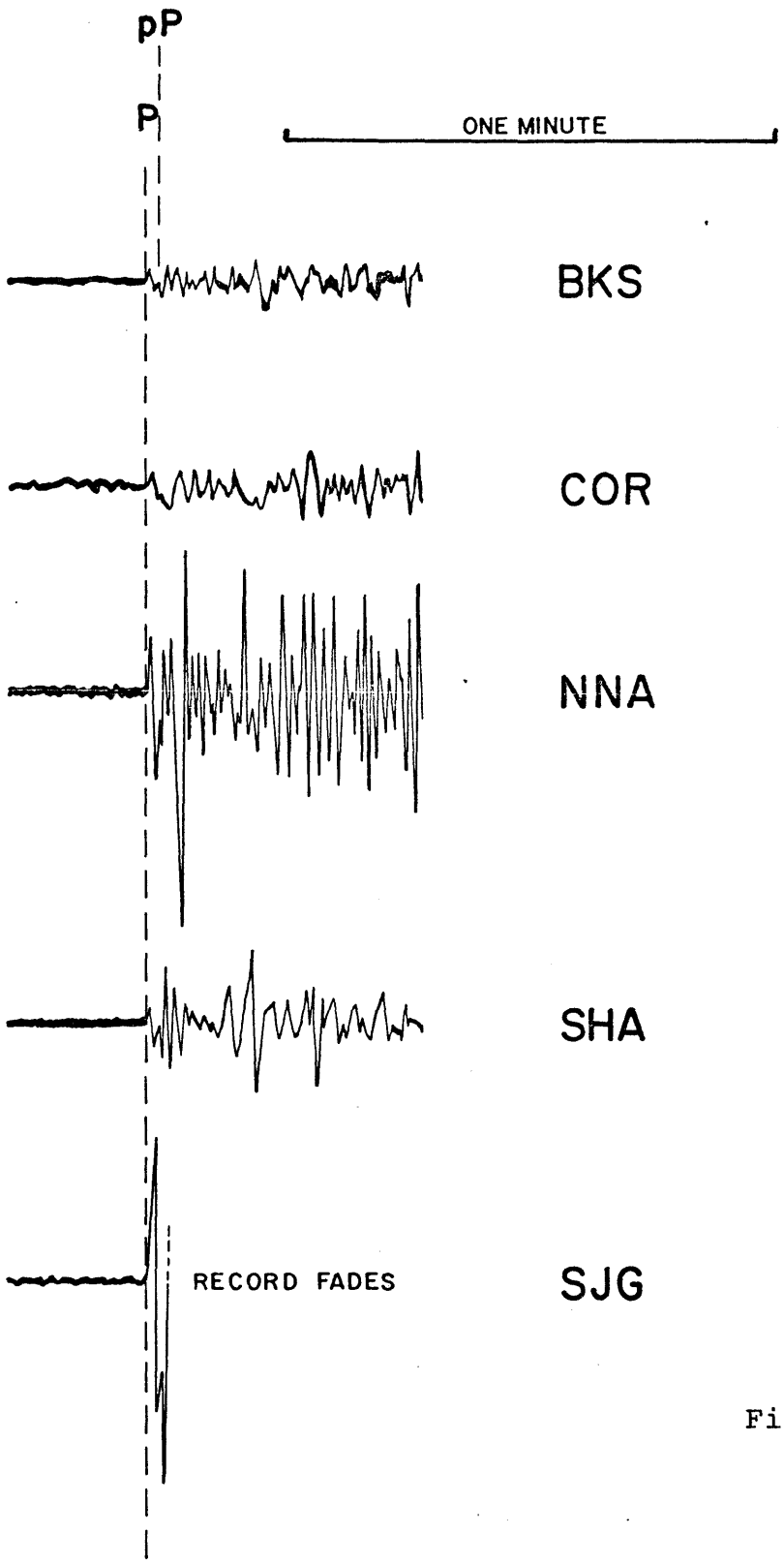

Figure 19.

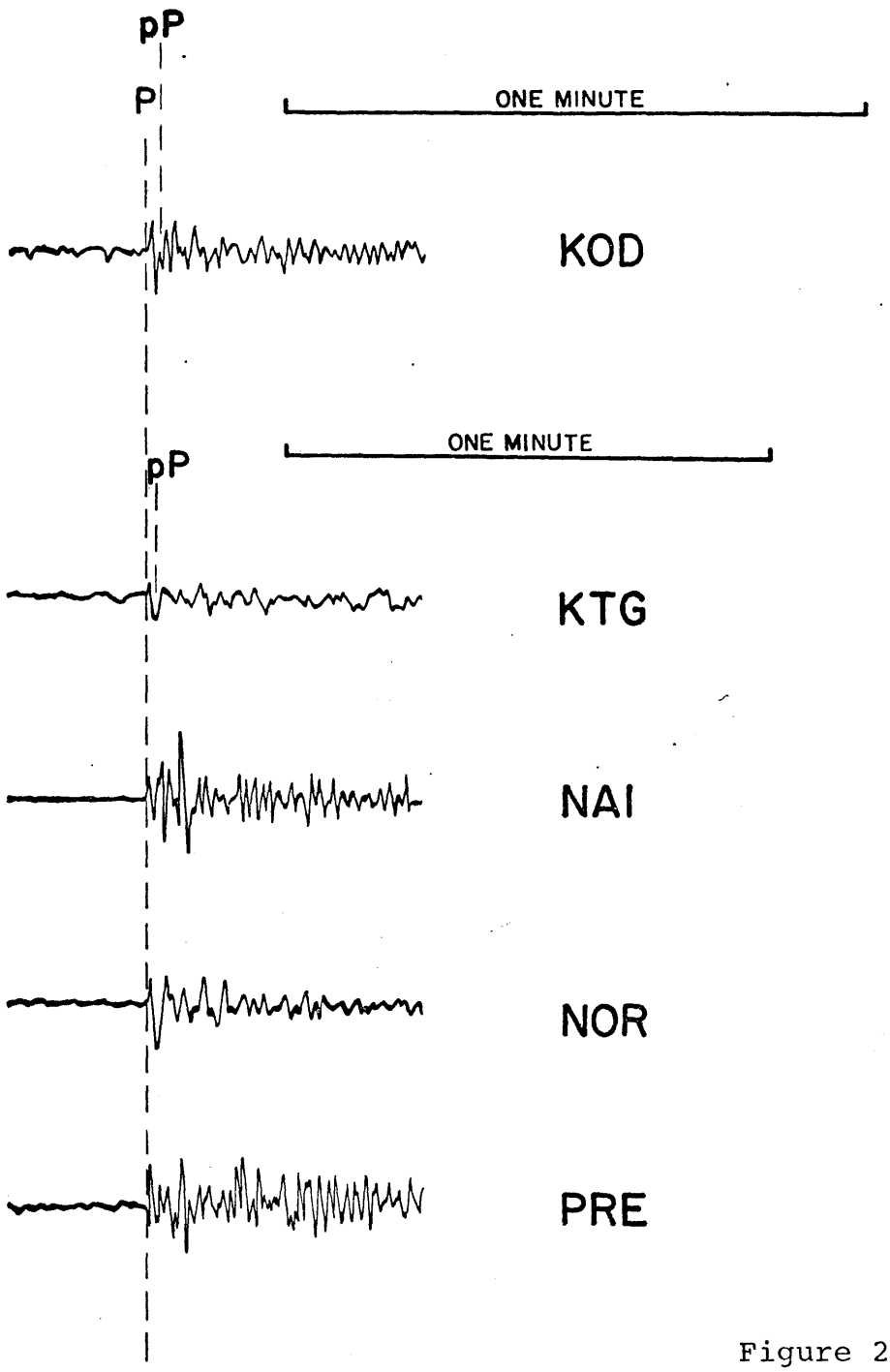

Figure 20.

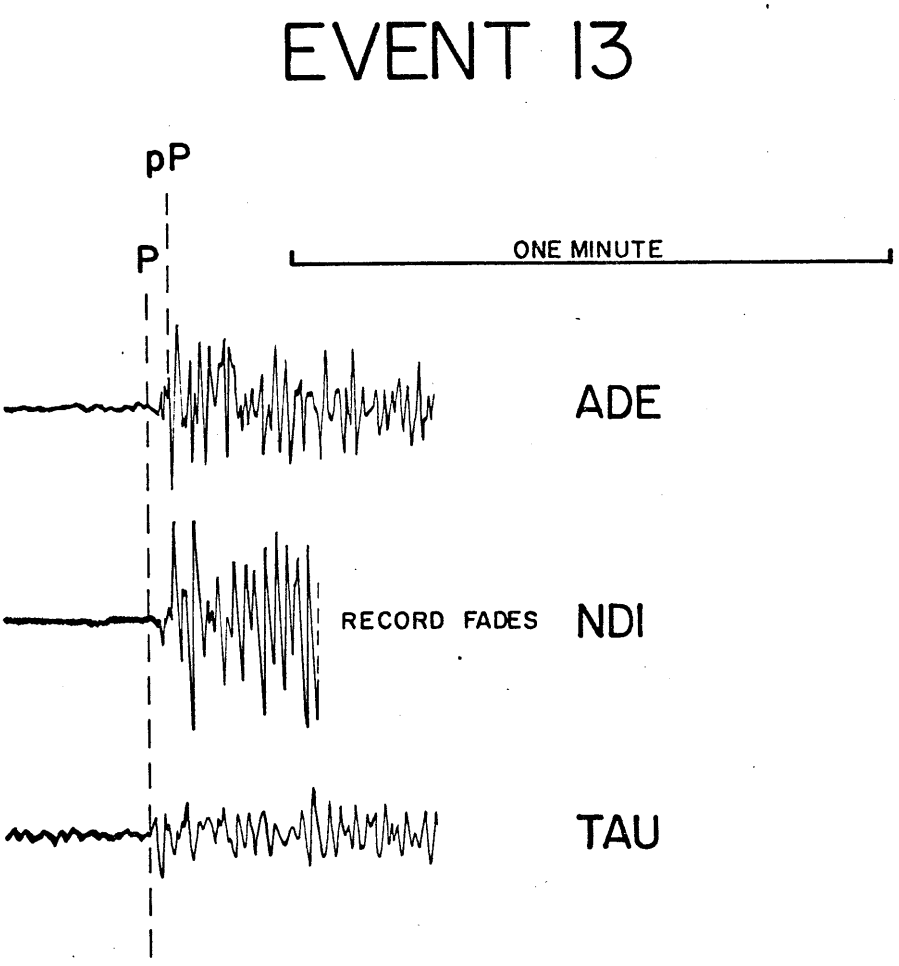

Figure 21.

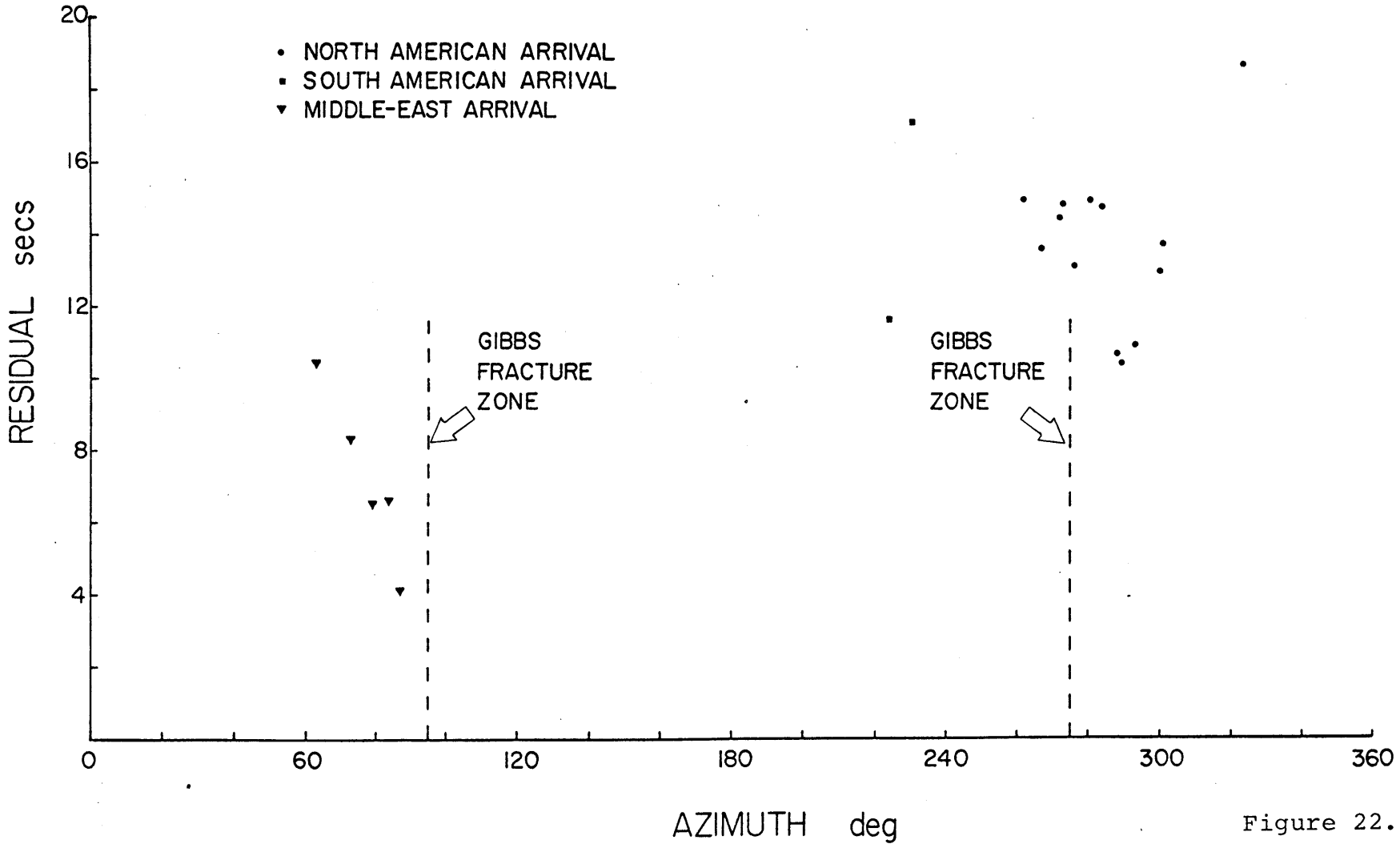
EVENT 25
NORTH AMERICAN ARRIVAL
SOUTH AMERICAN ARRIVAL
MIDDLE-EAST ARRIVAL
GIBBS FRACTURE ZONE
GIBBS FRACTURE ZONE
RESIDUAL secs
AZIMUTH deg
20
16
12
8
4
0
60
120
180
240
300
360

Figure 22.

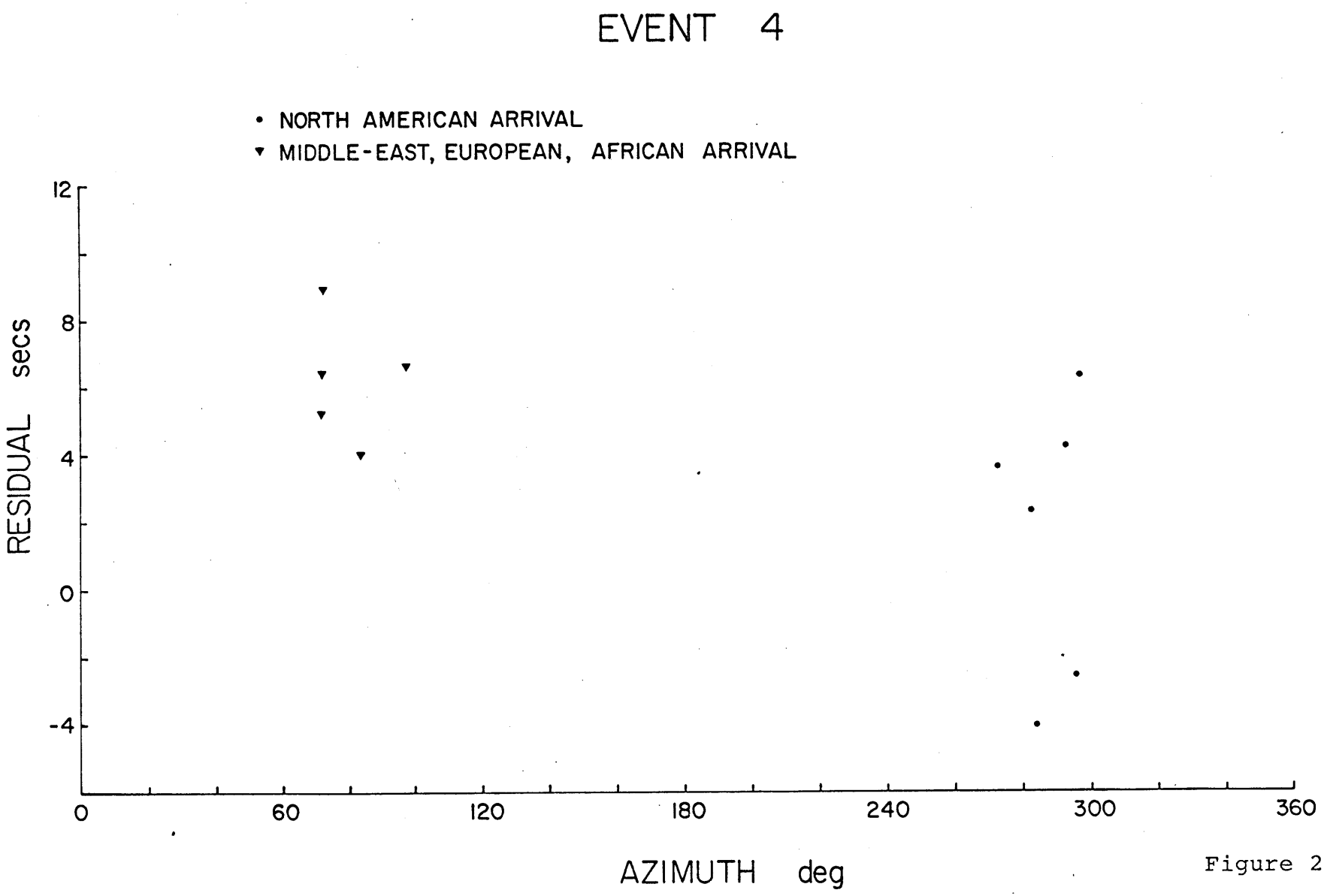
EVENT 4
• NORTH AMERICAN ARRIVAL
▼ MIDDLE-EAST, EUROPEAN, AFRICAN ARRIVAL
RESIDUAL secs
12
8
4
0
-4
0
60
120
180
240
300
360
AZIMUTH deg

Figure 23.

APPENDIX 1

One of the corrections applied to the residuals, not accounted for in the Jeffreys-Bullen travel time tables, is for ellipticity of the earth. Bullen (1937) has published a series of ellipticity corrections for epicenters between the latitudes 60°S and 60°N. By a very simple computation, this table has been extended to cover a wider range of latitudes.

The technique has been to use the back azimuth between points at latitudes higher than 60° to points at lower latitudes. For instance, the ellipticity correction for a wave, (not given in Bullen's table), originating at a latitude of 70°N and travelling 40° at an azimuth of 180° (ie. due south), is equivalent to the correction (given in Bullen's table) for a wave originating at a latitute of 30°N and travelling 40° at an azimuth of 000° (ie. due north). Similarly, the correction for a wave originating at a latitude of 70°N and travelling 40° at an azimuth of 60° is equivalent to that of a wave travelling 40° from a latitude of 56° at an azimuth of 328°.

In this manner, Bullen's table has been extended without involving any new calculations. In Table 4, the

extension of the tables is presented for the distance range 30° to 70°, which is of relevance to the present study. The blank spaces are those which cannot be computed by this method because both points between which the correction is being calculated lie at latitudes higher than 60°.

APPENDIX 2

Measured residuals, uncorrected and corrected for velocity heterogeneity below WWSSN stations, and for ellipticity of the earth, are presented on the following pages. Ratings are subjective, based on clarity of the seismogram, and sharpness of the shear wave arrival (see Figure 2).

EVENT NUMBER 1

DATE 9/20/69

ORIGIN TIME 5: 8:57.8

MAGNITUDE 5.6

LATITUDE 58.3500

LONGDITUDE -32.0800

NUMBER OF STATIONS REPORTING 22

STATION	DISTANCE (DEG)	AZIMUTH (DEG)	BACK AZIMUTH (DEG)	UNCORRECTED RESIDUAL (SEC)	CORRECTED RESIDUAL (SEC)	RATING
CAR	54.58	223.6	21.7	23.78	28.38	3
SCP	33.67	258.9	43.0	11.33	14.12	1
KBL	66.70	61.9	325.7	8.41	13.69	3
ATU	40.99	94.8	318.3	6.88	12.73	2
IST	41.52	87.1	315.9	7.83	12.52	2
EIL	53.40	92.2	322.8	6.87	11.75	3
SHA	46.75	258.9	36.9	7.92	11.52	3
HLW	51.26	95.1	322.8	7.75	11.37	1
JER	51.78	90.2	321.8	7.75	10.86	2
TRN	52.56	217.3	19.0	11.06	10.66	3
SJG	47.32	226.5	23.7	6.55	10.02	1
TAB	52.75	76.3	319.5	8.22	9.63	2
ATL	42.62	257.6	38.0	6.16	9.18	2
BEC	34.03	234.5	30.5	7.17	8.95	3
TUC	57.35	279.5	37.9	8.67	7.48	2
QUE	69.30	66.1	326.2	5.55	7.35	4
DAL	49.58	268.4	38.8	4.05	6.75	2
COL	47.86	328.8	39.8	4.54	6.36	3
LON	51.78	298.9	42.2	4.32	5.98	3
COR	54.10	298.1	40.6	7.45	5.80	1
DUG	52.32	287.2	41.1	4.97	3.62	2
GOL	48.89	281.3	42.1	2.29	2.87	3

EVENT NUMBER 2

DATE 11/16/65

ORIGIN TIME 15:24:44.0

MAGNITUDE 5.9

LATITUDE 31.0000

LONGDITUDE -41.5300

NUMBER OF STATIONS REPORTING 27

STATION	DISTANCE (DEG)	AZIMUTH (DEG)	BACK AZIMUTH (DEG)	UNCORRECTED RESIDUAL (SEC)	CORRECTED RESIDUAL (SEC)	RATING
COR	63.49	307.8	71.7	13.39	11.00	3
DAL	46.48	287.5	76.7	8.62	10.57	2
KTG	40.95	9.9	206.0	9.23	10.54	4
ATL	36.11	285.4	81.9	8.05	10.36	2
AAM	35.30	300.6	94.6	7.45	9.71	4
KEV	53.86	23.7	261.7	5.08	9.67	1
CAR	31.16	234.6	45.4	5.60	9.54	1
GOL	51.82	298.2	78.7	9.63	9.45	1
COP	44.89	40.5	259.7	5.70	9.11	2
IST	56.51	58.8	283.9	5.09	9.03	1
ATU	53.26	63.6	283.3	3.90	9.00	4
SDB	69.90	122.4	311.4	6.83	8.42	3
SJG	25.74	245.8	55.5	5.52	8.36	2
KON	44.36	34.5	253.1	5.25	8.02	2
JER	64.12	67.1	291.7	5.54	7.84	3
TUC	57.98	290.9	71.3	9.72	7.75	3
HLW	61.74	70.5	291.3	4.80	7.60	3
NOR	51.57	4.5	207.4	4.88	7.46	1
GIE	55.99	245.1	51.2	11.66	7.40	2
NUR	51.91	35.1	266.5	2.33	7.19	2
ALQ	53.76	292.7	74.6	8.55	7.07	1
LUB	50.44	289.8	75.4	6.88	6.39	1
GSC	61.75	296.1	70.5	10.35	6.02	4
GDH	38.91	353.2	163.5	2.79	5.81	2
QUI	46.82	235.6	45.1	7.14	5.63	3
NNA	54.56	224.0	37.5	1.85	-1.77	3
RCC	49.54	303.5	83.4	0.24	-2.32	3

EVENT NUMBER 3

DATE 6/ 2/65

ORIGIN TIME 23:40:23.1

MAGNITUDE 5.8

LATITUDE 15.9300

LONGDITUDE -46.6900

NUMBER OF STATIONS REPORTING 29

STATION	DISTANCE (DEG)	AZIMUTH (DEG)	BACK AZIMUTH (DEG)	UNCORRECTED RESIDUAL (SEC)	CORRECTED RESIDUAL (SEC)	RATING
TRI	58.20	45.8	260.0	8.14	11.20	2
KEV	69.53	20.9	260.3	6.49	10.89	2
ESK	51.48	30.2	237.8	8.92	10.82	3
COP	59.71	34.3	253.0	7.38	10.63	1
SHA	40.56	298.7	101.7	7.70	10.32	2
NUR	67.09	30.6	261.7	4.60	9.29	2
AAM	41.13	317.3	118.4	7.10	9.17	2
OGD	34.79	321.6	127.8	6.24	8.97	3
GEO	35.09	316.7	122.2	8.25	8.93	3
KON	59.61	29.3	248.1	6.00	8.61	3
DAL	48.18	299.9	98.0	6.89	8.60	1
TUC	59.93	298.3	89.5	10.13	7.84	3
OXF	42.48	303.9	104.9	4.88	7.54	1
VAL	46.10	30.7	232.5	6.05	7.51	2
GOL	55.99	307.3	97.5	7.91	7.50	2
WES	33.79	326.3	133.9	5.32	6.63	2
LUB	52.50	300.3	95.4	7.11	6.35	3
ATU	65.03	55.2	271.1	1.07	5.82	2
COR	69.51	312.1	87.6	8.21	5.51	2
ALO	56.39	301.5	93.6	7.23	5.48	2
SDB	66.95	114.2	294.8	4.21	5.47	2
ATL	38.13	304.2	107.9	3.35	5.42	2
JCT	50.49	296.5	94.2	6.63	5.11	1
LON	68.41	314.4	89.5	3.26	3.92	3
PTO	41.35	44.9	243.9	3.97	3.56	2
MAI	42.75	52.8	252.4	2.91	3.49	4
RCD	55.14	312.9	102.1	5.81	3.03	2
PEL	53.91	205.0	29.0	0.19	2.46	4
TCL	44.05	48.6	249.6	3.92	-0.79	2

EVENT NUMBER 4

DATE 9/17/64

ORIGIN TIME 15: 2: 1.5

MAGNITUDE 5.5

LATITUDE 44.58CC

LONGCITUCE -31.3400

NUMBER OF STATIONS REPORTING 11

STATION	DISTANCE (DEG)	AZIMUTH (DEG)	BACK AZIMUTH (DEG)	UNCORRECTED RESIDUAL (SEC)	CORRECTED RESIDUAL (SEC)	RATING
IST	43.52	72.6	295.6	4.56	8.88	2
AAE	69.56	97.6	314.2	12.82	6.64	3
SHI	65.75	71.7	308.8	3.13	6.38	1
DUG	57.94	296.6	56.5	8.04	6.26	2
TRI	31.52	71.7	284.4	1.65	5.19	3
MNN	42.97	293.2	67.6	2.64	4.19	1
HLW	50.85	84.4	305.0	0.84	4.02	3
ATL	41.99	273.4	58.5	0.97	3.57	1
FLO	43.62	283.8	62.6	-0.20	2.33	2
RCD	49.82	296.3	62.7	-0.35	-2.56	3
LUB	54.27	284.2	56.1	-3.88	-4.05	4

EVENT NUMBER 5

DATE 9/ 3/68

ORIGIN TIME 15:37: 0.3

MAGNITUDE 5.6

LATITUDE 20.5800

LONGDITUDE -62.3000

NUMBER OF STATIONS REPORTING 17

STATION	DISTANCE (DEG)	AZIMUTH (DEG)	BACK AZIMUTH (DEG)	UNCORRECTED RESIDUAL (SEC)	CORRECTED RESIDUAL (SEC)	RATING
UME	68.46	28.2	272.8	10.53	13.35	3
KBS	66.91	11.7	258.6	1.57	6.64	2
TUC	44.62	295.5	92.8	7.35	5.22	2
PEL	54.02	188.7	9.7	2.18	4.59	3
KTG	55.26	15.4	227.5	3.25	4.39	4
COP	64.68	37.2	269.7	0.74	3.97	2
TRI	65.96	48.1	275.3	0.61	3.62	1
ALQ	41.28	299.8	98.4	2.17	0.53	2
DUG	47.08	306.2	99.1	2.23	-0.03	2
ESK	55.82	36.4	256.4	-3.28	-1.38	3
COL	69.67	333.0	85.0	-2.51	-1.48	2
PTO	49.61	53.1	262.5	-1.36	-1.76	2
COR	55.32	310.5	94.7	0.77	-1.78	3
GDH	48.97	4.1	190.9	-4.79	-1.87	3
NOR	63.77	6.7	228.3	-4.42	-2.00	4
VAL	50.86	39.0	252.3	-3.77	-2.29	2
NNA	35.38	205.1	24.0	-2.76	-6.49	2

EVENT NUMBER 6

DATE 10/23/64

ORIGIN TIME 1:56: 5.1

MAGNITUDE 6.2

LATITUDE 19.8000

LONGDITUDE -56.1100

NUMBER OF STATIONS REPORTING 19

STATION	DISTANCE (DEG)	AZIMUTH (DEG)	BACK AZIMUTH (DEG)	UNCORRECTED RESIDUAL (SEC)	CORRECTED RESIDUAL (SEC)	RATING
GDH	49.47	1.2	183.2	13.13	16.07	1
VAL	47.90	36.8	245.6	7.47	8.95	2
TOL	48.66	53.9	261.5	11.11	6.41	1
COP	61.80	36.7	263.9	2.21	5.46	3
FLO	35.09	310.1	112.8	3.30	5.33	2
BKS	59.51	302.9	87.8	7.51	5.32	1
GOL	46.50	306.3	100.4	5.64	5.30	1
MAL	47.98	58.1	264.1	4.64	5.20	2
OXF	32.88	303.4	107.8	2.21	4.93	2
TUC	50.19	295.9	90.3	6.45	4.30	1
QUI	29.61	230.4	46.6	4.27	2.64	3
COR	60.24	310.6	91.0	4.37	1.78	1
LUB	42.79	298.3	96.8	1.78	1.10	1
LON	59.27	313.2	93.3	-0.18	0.57	1
PEL	54.46	195.0	16.9	-1.86	0.51	1
DAL	38.47	298.1	99.4	-2.44	-0.67	2
ALQ	46.72	299.7	95.2	-0.11	-1.77	2
NNA	37.61	214.6	33.1	-1.99	-5.80	2
ARE	39.08	203.8	23.3	-3.33	-8.03	1

EVENT NUMBER 7

DATE 10/20/72

ORIGIN TIME 4:33:49.9

MAGNITUDE 5.7

LATITUDE 20.6000

LONGDITUDE -29.6900

NUMBER OF STATIONS REPORTING 24

STATION	DISTANCE (DEG)	AZIMUTH (DEG)	BACK AZIMUTH (DEG)	UNCORRECTED RESIDUAL (SEC)	CORRECTED RESIDUAL (SEC)	RATING
GIE	62.92	258.1	66.5	17.33	12.70	2
ALQ	67.94	300.4	79.7	12.50	10.62	3
SJG	34.44	272.2	79.8	3.98	6.53	1
SCP	45.42	307.4	101.4	4.23	6.19	2
NAI	68.54	99.9	292.6	11.34	4.61	3
HLW	55.43	67.4	275.5	1.11	3.71	1
BLA	46.84	302.1	96.1	3.41	3.59	2
ATU	49.03	57.2	265.0	-1.75	3.20	1
OGD	43.08	308.6	104.4	0.38	3.10	3
LPS	56.83	273.9	74.6	4.49	2.87	1
IST	53.34	53.7	266.1	-1.05	2.73	1
WIN	62.65	130.7	309.8	3.01	2.48	2
AAM	49.96	308.4	98.3	0.22	2.31	1
BHP	49.41	264.1	70.6	2.98	1.77	1
CAR	37.17	260.1	69.8	-2.03	1.61	2
BUL	69.95	121.7	302.0	1.38	1.52	2
ANT	59.27	224.1	45.3	1.05	1.01	2
TRI	43.44	44.5	249.6	-2.20	0.92	3
TAB	66.83	56.4	278.6	0.55	0.85	1
VAL	34.75	21.2	213.2	-2.09	-0.64	1
ESK	39.98	23.4	220.6	-4.35	-2.48	2
ATL	49.83	296.8	90.4	-4.73	-2.67	3
JCT	63.15	294.5	80.9	-1.06	-2.68	2
ARE	55.14	231.2	49.6	-1.70	-6.54	3

EVENT NUMBER 8

DATE 9/30/71

ORIGIN TIME 21:24:10.8

MAGNITUDE 6.0

LATITUDE -0.4500

LONGDITUDE -4.8900

NUMBER OF STATIONS REPORTING 19

STATION	DISTANCE (DEG)	AZIMUTH (DEG)	BACK AZIMUTH (DEG)	UNCORRECTED RESIDUAL (SEC)	CORRECTED RESIDUAL (SEC)	RATING
BEC	65.07	306.3	107.6	11.13	11.76	2
EIL	48.30	48.4	239.1	4.48	8.30	2
IST	51.48	32.6	225.4	3.02	6.84	3
NUR	64.93	15.6	213.0	1.50	6.15	2
COP	57.71	11.5	200.6	2.00	5.26	2
ATU	46.45	31.5	221.3	0.12	5.09	1
KON	61.00	8.4	196.7	1.70	4.31	2
SHI	62.29	55.9	252.1	1.64	4.11	2
HLW	45.83	45.7	235.5	1.18	3.77	1
VAL	52.39	355.8	173.2	1.24	2.74	3
TRN	57.25	282.9	97.4	3.99	2.22	2
CAR	62.63	282.0	96.0	-1.31	1.85	1
ESK	55.60	1.2	182.0	-1.49	0.48	2
ANT	67.49	244.6	80.1	0.35	-0.15	1
SJG	62.94	290.5	110.1	-2.51	-0.39	3
WIN	30.68	137.3	312.8	-0.93	-1.51	2
PRE	40.62	130.9	303.0	-1.86	-2.46	2
NAI	41.70	91.4	270.7	4.01	-2.68	2
ARE	67.47	252.4	83.5	-2.07	-7.33	2

EVENT NUMBER 9

DATE 3/31/70

ORIGIN TIME 18:13:28.0

MAGNITUDE 5.5

LATITUDE -3.7800

LONGDITUDE 69.7000

NUMBER OF STATIONS REPORTING 18

STATION	DISTANCE (DEG)	AZIMUTH (DEG)	BACK AZIMUTH (DEG)	UNCORRECTED RESIDUAL (SEC)	CORRECTED RESIDUAL (SEC)	RATING
KBL	38.12	359.1	178.9	5.70	10.26	2
JER	48.23	319.7	130.7	7.34	9.60	2
CHG	36.52	51.1	235.1	7.78	8.23	1
SHL	36.25	35.2	219.6	5.09	6.92	2
MUN	51.82	128.3	292.9	4.85	6.45	2
IST	58.04	324.5	129.9	0.98	4.90	2
TAB	46.94	334.6	147.2	3.90	4.54	1
BAG	54.13	66.8	252.8	5.26	3.99	2
MSH	40.99	347.5	164.5	4.16	3.95	1
QUE	33.88	355.7	175.1	1.97	3.00	3
HKC	50.60	57.1	244.8	6.79	2.65	2
ATU	59.48	318.7	123.6	-2.64	2.36	2
WIN	54.18	244.9	77.8	2.94	2.06	2
MAN	54.11	69.0	254.2	3.93	1.43	3
AAE	33.36	292.6	111.1	7.31	0.67	1
PRE	45.40	237.1	68.3	1.14	0.39	2
NDI	33.08	12.2	193.8	-4.48	-1.32	3
NAI	32.96	273.5	95.0	3.93	-2.62	1

EVENT NUMBER 10

DATE 3/ 2/68

ORIGIN TIME 22: 2:24.2

MAGNITUDE 5.5

LATITUDE -6.0900

LONGDITUDE 71.4100

NUMBER OF STATIONS REPORTING 12

STATION	DISTANCE (DEG)	AZIMUTH (DEG)	BACK AZIMUTH (DEG)	UNCORRECTED RESIDUAL (SEC)	CORRECTED RESIDUAL (SEC)	RATING
WIN	54.80	246.7	81.3	14.17	13.27	3
JER	51.09	319.7	131.0	7.93	10.27	2
QUE	36.32	353.5	172.5	7.16	8.28	3
LEM	35.98	93.2	269.0	4.39	5.89	3
SHL	37.23	31.5	215.1	3.61	5.55	1
TAB	49.75	334.0	146.5	4.29	5.04	1
MSH	43.61	346.1	162.8	3.23	3.13	2
BAG	53.53	64.6	249.3	4.27	3.10	2
LAH	37.53	4.1	184.8	0.79	3.07	1
NDI	35.02	8.9	190.1	-0.36	2.89	2
MUN	49.06	127.6	291.9	0.31	1.87	3
NAI	34.85	276.5	98.8	0.85	-5.66	3

EVENT NUMBER 11

DATE 9/12/65

ORIGIN TIME 22: 2:37.7

MAGNITUDE 6.1

LATITUDE -6.4600

LONGDITUDE 70.7600

NUMBER OF STATIONS REPORTING 20

STATION	DISTANCE (DEG)	AZIMUTH (DEG)	BACK AZIMUTH (DEG)	UNCORRECTED RESIDUAL (SEC)	CORRECTED RESIDUAL (SEC)	RATING
SDB	56.69	256.4	88.0	7.79	8.95	1
AAE	35.41	295.4	114.7	14.07	7.49	2
IST	60.82	324.8	130.7	2.61	6.63	3
ANP	58.51	55.4	244.5	6.06	6.09	4
TAB	49.80	334.7	147.4	4.90	5.66	1
SHL	37.88	32.0	215.7	3.71	5.66	4
MUN	49.35	127.0	291.0	3.70	5.25	1
ADE	68.27	125.0	277.5	3.62	5.08	1
HOW	33.45	30.4	212.9	6.78	4.80	2
WIN	54.06	246.9	81.4	5.28	4.38	2
NDI	35.49	9.8	191.1	0.88	4.14	2
ATJ	62.18	319.2	124.7	-1.21	3.86	3
HKC	51.22	54.7	241.2	7.23	3.21	3
LAH	37.95	5.0	185.8	0.90	3.18	2
PRE	44.91	239.8	72.2	2.80	2.02	2
BUL	43.07	247.4	77.6	1.37	1.47	1
SHI	39.95	334.9	151.0	-2.37	0.63	4
SFO	68.20	45.3	242.8	1.13	-1.27	4
CHG	37.46	47.4	230.6	-3.83	-3.28	4
NAI	34.26	277.2	99.6	-0.98	-7.48	2

EVENT NUMBER 12

DATE 12/ 3/64

ORIGIN TIME 3:50: 1.7

MAGNITUDE 5.7

LATITUDE -14.8400

LONGDITUDE 66.7600

NUMBER OF STATIONS REPORTING 9

STATION	DISTANCE (DEG)	AZIMUTH (DEG)	BACK AZIMUTH (DEG)	UNCORRECTED RESIDUAL (SEC)	CORRECTED RESIDUAL (SEC)	RATING
SDB	51.30	262.6	97.2	11.69	12.91	2
QUE	44.77	0.2	180.3	7.63	9.21	1
IST	65.68	329.4	139.5	4.50	8.85	3
HOW	42.62	30.1	211.6	8.73	7.10	1
SHL	47.03	31.6	214.1	3.23	5.54	4
HKC	59.33	52.4	235.9	8.86	5.06	3
AAE	36.51	308.8	130.3	10.65	4.39	3
CHG	46.08	44.5	225.7	2.86	3.72	2
NHA	49.90	59.6	238.6	6.97	3.28	2

EVENT NUMBER 13

DATE 10/10/70

ORIGIN TIME 8:53: 4.5

MAGNITUDE 5.8

LATITUDE -3.5600

LONGDITUDE 86.1900

NUMBER OF STATIONS REPORTING 18

STATION	DISTANCE (DEG)	AZIMUTH (DEG)	BACK AZIMUTH (DEG)	UNCORRECTED RESIDUAL (SEC)	CORRECTED RESIDUAL (SEC)	RATING
NDI	33.20	345.5	163.5	10.39	13.53	2
ANP	44.63	48.2	235.2	8.81	8.92	2
NIL	38.98	342.7	159.2	5.91	7.45	2
HKC	37.53	45.5	230.2	7.58	3.62	3
TAU	66.68	135.5	287.9	2.62	3.01	1
EIL	59.06	307.6	114.8	-0.98	2.85	3
QUE	38.27	332.6	147.9	1.74	2.71	3
JER	59.82	310.0	116.2	0.16	2.27	1
PMG	60.79	98.7	271.2	3.02	2.17	1
SHI	46.15	318.0	129.9	-0.69	2.12	3
ADE	57.72	129.6	290.5	-0.96	0.61	2
AAE	48.90	285.1	102.7	6.00	-0.84	1
RIV	67.31	125.2	281.4	1.70	-0.96	1
IST	68.37	316.8	115.5	-4.86	-1.11	2
MUN	39.92	138.5	308.9	-2.87	-1.13	1
BAG	39.36	58.7	242.7	-0.23	-1.31	2
RAB	65.82	93.0	268.0	-1.80	-2.77	2
TAB	55.47	322.1	129.1	-5.41	-4.85	3

EVENT NUMBER 14

DATE 5/25/64

ORIGIN TIME 19:44: 5.9

MAGNITUDE 5.7

LATITUDE -9.0800

LONGDITJDE 88.8900

NUMBER OF STATIONS REPORTING 8

STATION	DISTANCE (DEG)	AZIMUTH (DEG)	BACK AZIMUTH (DEG)	UNCORRECTED RESIDUAL (SEC)	CORRECTED RESIDUAL (SEC)	RATING
HKC	39.84	38.1	221.2	11.42	7.67	3
BAG	40.31	51.2	233.3	7.00	6.13	1
SHL	34.56	4.8	185.2	2.61	4.72	1
SHI	52.03	319.1	132.0	0.88	3.90	3
PMG	57.45	95.4	265.2	3.85	3.02	1
LAH	42.74	341.6	158.5	-0.20	2.15	1
NDI	39.20	343.7	161.6	-1.61	1.72	2
NAI	52.40	275.4	100.4	0.80	-5.92	3

EVENT NUMBER 15

DATE 6/26/71

ORIGIN TIME 19:27:11.0

MAGNITUDE 5.9

LATITUDE -5.1800

LONGDITUDE 96.9000

NUMBER OF STATIONS REPORTING 11

STATION	DISTANCE (DEG)	AZIMUTH (DEG)	BACK AZIMUTH (DEG)	UNCORRECTED RESIDUAL (SEC)	CORRECTED RESIDUAL (SEC)	RATING
EIL	68.65	304.3	109.3	-0.60	3.15	2
JER	69.20	306.7	110.3	0.93	2.94	2
HKC	32.12	31.1	213.8	5.79	1.99	2
SHI	54.86	311.9	121.6	-0.86	1.92	3
MSH	54.06	322.8	131.8	2.03	1.81	3
MUN	32.21	148.2	321.8	-0.41	1.35	2
BUL	67.86	250.5	87.4	0.73	0.64	2
PRE	68.60	244.5	85.4	-0.26	-1.17	1
NDI	38.63	331.7	147.5	-4.58	-1.41	3
NAI	60.11	271.5	95.2	3.83	-3.07	2
ADE	48.63	133.2	297.8	-5.58	-4.03	3

EVENT NUMBER 16

DATE 2/17/66

ORIGIN TIME 11:47:57.3

MAGNITUDE 6.0

LATITUDE -32.2000

LONGDITUDE 78.9300

NUMBER OF STATIONS REPORTING 16

STATION	DISTANCE (DEG)	AZIMUTH (DEG)	BACK AZIMUTH (DEG)	UNCORRECTED RESIDUAL (SEC)	CORRECTED RESIDUAL (SEC)	RATING
CTA	60.77	96.4	243.7	8.05	9.10	2
MUN	31.48	99.7	259.5	6.94	8.97	3
WIN	55.09	263.6	114.3	8.37	7.85	2
BUL	46.35	272.2	115.6	6.38	6.94	3
POO	50.68	353.8	174.4	2.49	5.97	2
AAE	56.13	309.9	138.8	11.49	5.76	3
KOO	42.22	357.9	178.2	4.85	5.64	2
NDI	60.57	358.3	178.3	1.19	5.57	2
SHL	58.76	13.7	192.8	2.34	5.40	3
RIV	59.38	112.9	249.7	7.63	5.12	3
HKC	63.82	36.5	213.0	7.34	4.38	1
PMG	66.64	86.5	239.0	4.46	4.07	2
NHA	52.82	38.2	212.5	6.64	3.91	1
QUE	63.08	348.4	168.6	1.45	3.58	1
PRE	44.52	264.8	110.6	3.65	3.28	3
LAH	63.55	355.6	175.6	-1.47	1.87	3

EVENT NUMBER 17

DATE 12/19/65

ORIGIN TIME 22: 6:33.0

MAGNITUDE 5.5

LATITUDE -32.2400

LONGDITUDE 78.8700

NUMBER OF STATIONS REPORTING 23

STATION	DISTANCE (DEG)	AZIMUTH (DEG)	BACK AZIMUTH (DEG)	UNCORRECTED RESIDUAL (SEC)	CORRECTED RESIDUAL (SEC)	RATING
NAI	50.15	299.3	132.3	14.77	9.08	3
ADE	49.26	110.4	255.2	7.29	8.96	2
SDB	61.43	269.8	118.8	6.94	8.50	2
BUL	46.31	272.3	115.7	6.66	7.23	2
SBA	58.30	165.6	264.5	9.10	6.02	2
CTA	60.82	96.4	243.6	4.64	5.69	1
CHG	54.27	23.7	201.0	3.65	5.43	1
RIV	59.42	112.9	249.7	7.77	5.26	2
POO	50.71	353.8	174.5	1.78	5.26	1
AAE	56.12	310.0	138.9	10.58	4.86	1
HOW	55.09	10.7	189.8	5.51	4.72	3
BAG	62.73	45.9	219.4	4.64	4.48	2
SHL	58.81	13.8	192.9	1.13	4.19	1
SHI	66.43	335.1	155.8	-1.20	2.73	2
NHA	52.88	38.3	212.5	5.42	2.70	1
TAU	53.93	122.3	257.2	2.25	2.53	2
WIN	55.03	263.6	114.3	2.92	2.41	3
PRE	44.47	264.9	110.6	2.46	2.09	3
MAN	61.71	47.6	220.3	3.35	1.95	3
PMG	66.70	86.5	239.0	2.32	1.93	2
QUE	63.11	348.4	168.7	-0.53	1.60	3
HKC	63.89	36.6	213.1	4.40	1.44	2
LAH	63.59	355.7	175.7	-2.70	0.64	2

EVENT NUMBER 18

DATE 10/ 8/68

ORIGIN TIME 7:43:22.8

MAGNITUDE 5.8

LATITUDE -39.8500

LONGDITUDE 87.7400

NUMBER OF STATIONS REPORTING 13

STATION	DISTANCE (DEG)	AZIMUTH (DEG)	BACK AZIMUTH (DEG)	UNCORRECTED RESIDUAL (SEC)	CORRECTED RESIDUAL (SEC)	RATING
SHL	65.19	4.1	183.5	7.94	11.21	3
SDB	68.51	268.2	127.3	8.38	10.10	2
WIN	61.35	263.6	124.1	9.97	9.61	2
HKC	66.57	26.7	201.9	9.32	6.67	3
RIV	50.18	104.2	243.7	8.56	6.37	1
BUL	53.87	273.1	125.1	5.56	6.31	4
ADE	40.33	99.7	247.5	3.03	5.05	1
NAT	60.06	296.4	136.4	9.15	3.52	3
SPA	50.34	180.0	87.7	1.87	3.51	1
PRF	51.12	267.0	121.5	2.69	2.51	3
NHA	55.51	25.7	200.0	3.56	1.24	1
POD	59.51	344.7	167.6	-3.43	0.06	2
CTA	53.43	86.4	234.8	-3.05	-1.58	1

EVENT NUMBER 19

DATE 1/21/70

ORIGIN TIME 17:51:37.4

MAGNITUDE 6.1

LATITUDE 7.0300

LONGDITUDE -104.2400

NUMBER OF STATIONS REPORTING 7

STATION	DISTANCE (DEG)	AZIMUTH (DEG)	BACK AZIMUTH (DEG)	UNCORRECTED RESIDUAL (SEC)	CORRECTED RESIDUAL (SEC)	RATING
ARE	39.93	126.0	303.2	17.22	12.33	2
KIP	53.79	291.3	97.1	13.69	10.52	2
COL	65.37	341.1	131.2	7.66	8.59	1
GOL	32.54	358.4	177.9	7.60	7.31	2
BEC	44.58	50.2	244.2	6.31	7.12	3
SCP	41.05	30.9	222.2	4.67	6.62	3
LON	42.36	342.1	153.6	1.51	2.25	4

EVENT NUMBER 20

DATE 5/ 2/72

ORIGIN TIME 6:56:23.2

MAGNITUDE 5.9

LATITUDE 5.2200

LONGDITUDE -100.3200

NUMBER OF STATIONS REPORTING 15

STATION	DISTANCE (DEG)	AZIMUTH (DEG)	BACK AZIMUTH (DEG)	UNCORRECTED RESIDUAL (SEC)	CORRECTED RESIDUAL (SEC)	RATING
DUG	36.59	343.9	158.8	11.54	9.28	2
SJG	35.75	66.1	253.2	6.53	8.95	1
BEC	42.86	46.5	238.6	7.97	8.79	2
BKS	38.15	331.4	143.0	9.85	7.76	4
ATL	31.77	25.9	211.4	5.61	7.74	3
COR	44.08	336.4	146.0	10.00	7.44	4
ANT	40.96	135.8	310.8	7.35	7.20	4
GOL	34.63	353.1	171.1	7.47	7.17	3
SCP	40.76	26.4	215.6	4.40	6.35	1
WES	45.08	30.5	223.0	5.00	6.28	1
BLA	36.67	27.1	214.6	5.92	6.13	2
GEO	39.60	28.9	218.1	5.12	5.78	2
GSC	33.58	335.2	149.3	10.09	5.68	1
ARE	35.74	127.6	304.7	8.09	3.23	2
AAM	39.79	19.4	206.5	0.92	2.96	3

EVENT NUMBER 21

DATE 1/29/69

ORIGIN TIME 17:44:31.6

MAGNITUDE 6.0

LATITUDE -17.1500

LONGCITUDE -171.5700

NUMBER OF STATIONS REPORTING 8

STATION	DISTANCE (DEG)	AZIMUTH (DEG)	BACK AZIMUTH (DEG)	UNCORRECTED RESIDUAL (SEC)	CORRECTED RESIDUAL (SEC)	RATING
SBA	61.66	185.1	23.6	5.47	2.58	3
CTA	40.00	259.0	93.0	0.85	1.76	3
PMG	40.83	275.4	105.3	1.64	1.23	4
RAB	37.80	285.7	112.7	0.73	0.51	4
DAV	66.61	285.8	112.0	3.18	0.11	2
ADE	47.56	238.1	81.3	-3.10	-1.76	2
TAU	43.27	224.8	66.5	-3.02	-2.91	2
RIV	37.28	236.3	72.9	-0.31	-3.00	1

EVENT NUMBER 22

DATE 11/12/67

ORIGIN TIME 10:36:51.0

MAGNITUDE 5.6

LATITUDE -17.1900

LONGCITUDE -171.9800

NUMBER OF STATIONS REPORTING 5

STATION	DISTANCE (DEG)	AZIMUTH (DEG)	BACK AZIMUTH (DEG)	UNCORRECTED RESIDUAL (SEC)	CORRECTED RESIDUAL (SEC)	RATING
MUN	65.90	242.2	95.8	0.66	2.08	1
ADE	47.20	238.1	81.0	-1.85	-0.51	1
TAU	42.97	224.7	66.1	-2.30	-2.18	2
CTA	39.61	259.1	92.9	-4.48	-3.57	2
RIV	36.93	236.2	72.6	-1.09	-3.77	1

EVENT NUMBER 23

DATE 5/ 9/71

ORIGIN TIME 8:25: 1.1

MAGNITUDE 6.0

LATITUDE -39.7800

LONGDITUDE -104.8700

NUMBER OF STATIONS REPORTING 7

STATION	DISTANCE (DEG)	AZIMUTH (DEG)	BACK AZIMUTH (DEG)	UNCORRECTED RESIDUAL (SEC)	CORRECTED RESIDUAL (SEC)	RATING
CAR	61.17	43.7	212.7	12.13	16.92	2
BHP	53.87	31.5	204.1	14.78	15.28	3
LPS	55.75	18.5	194.6	13.48	13.66	3
QUI	46.16	38.0	208.3	13.36	13.06	1
TRN	64.36	48.6	216.0	13.40	13.06	3
RAR	50.01	274.8	124.6	12.94	12.84	2
ARE	37.16	60.9	224.6	12.17	8.30	3

EVENT NUMBER 24

DATE 8/25/64

ORIGIN TIME 13:47:19.3

MAGNITUDE 6.2

LATITUDE 78.150C

LONGDITUDE 126.650C

NUMBER OF STATIONS REPORTING 28

STATION	DISTANCE (DEG)	AZIMUTH (DEG)	BACK AZIMUTH (DEG)	UNCORRECTED RESIDUAL (SEC)	CORRECTED RESIDUAL (SEC)	RATING
SEC	40.69	179.6	359.9	11.90	10.75	1
ALQ	62.88	47.6	349.3	10.37	9.97	3
TUC	64.77	52.1	348.9	10.19	9.33	1
JER	59.46	278.6	13.9	5.60	8.96	2
GDH	32.81	0.1	359.9	4.54	8.91	3
GOL	58.38	45.6	349.0	6.68	7.52	2
AAM	58.42	26.1	353.0	3.85	7.10	2
ESK	43.36	320.3	13.4	3.30	7.01	2
KON	37.33	311.7	17.7	2.69	6.98	3
PTO	57.97	321.2	9.9	5.26	6.04	2
DAL	66.31	39.2	351.1	1.32	4.38	3
ANP	53.09	185.8	1.3	2.77	4.20	1
OXF	65.55	32.3	352.3	-0.27	3.71	1
ATI	67.15	27.9	353.4	-0.04	3.36	3
HOW	58.60	222.3	8.6	3.68	2.68	1
MNN	54.85	33.8	350.7	0.30	2.54	2
MAL	61.74	316.5	10.2	-0.61	1.18	2
BAG	61.84	186.6	1.4	0.77	1.06	1
RCD	54.40	42.7	348.8	2.07	0.53	3
MAN	63.56	186.0	1.3	1.17	0.28	3
SHI	57.95	261.1	13.6	-3.72	0.25	3
NHA	66.52	198.6	3.9	2.09	-0.43	1
LUB	64.89	43.7	350.2	-1.26	-0.67	2
HKC	56.22	193.9	3.1	1.76	-0.97	2
NDI	54.18	235.4	11.2	-5.50	-1.27	3
CHG	60.88	210.2	6.3	-3.05	-1.41	3
TOL	58.59	316.9	10.6	1.15	-2.37	2
COR	50.67	60.2	345.5	-5.36	-6.68	3

EVENT NUMBER 25

DATE 2/13/67

ORIGIN TIME 23:14:22.3

MAGNITUDE 5.6

LATITUDE 52.8200

LONGDITUDE -34.2500

NUMBER OF STATIONS REPORTING 20

STATION	DISTANCE (DEG)	AZIMUTH (DEG)	BACK AZIMUTH (DEG)	UNCORRECTED RESIDUAL (SEC)	CORRECTED RESIDUAL (SEC)	RATING
CMC	39.47	323.9	70.5	15.47	18.61	3
QUI	64.41	230.7	28.0	18.06	17.13	4
ATL	40.41	261.7	45.9	12.10	14.94	1
ALQ	52.74	280.6	46.6	15.79	14.90	2
FLO	40.51	272.9	50.9	12.06	14.80	2
GOL	48.92	284.4	49.6	14.35	14.75	1
AAM	34.32	272.4	54.8	11.71	14.46	3
LON	53.50	301.3	49.0	12.29	13.79	3
OXF	42.73	267.2	47.2	10.26	13.69	1
LUB	50.91	276.0	46.3	13.04	13.10	2
COR	55.73	300.2	47.3	14.74	12.91	4
CAR	49.73	224.1	25.4	7.24	11.67	4
BKS	59.81	293.8	44.6	12.29	10.92	3
GSC	58.56	288.1	44.9	14.37	10.65	2
DUG	52.91	289.7	48.2	12.02	10.49	2
MSH	64.17	63.6	317.7	10.05	10.42	1
SHI	65.11	73.4	318.1	4.82	8.32	1
JER	53.28	84.2	314.8	3.72	6.63	2
IST	43.40	79.4	307.9	2.03	6.57	2
ATU	42.15	86.7	309.9	-1.54	4.14	3